DOI:10.1130/B31xxx.1

†eric.portenga@emich.edu
§Present address: Department of Earth and Environmental Science, Norwich University, Northfield, Vermont 05663, USA.

GSA Bulletin; Month/Month 2016; v. 128; no. X/X; p. 000–000; doi: 10.1130/B31xxx.1; 12 figures; 1 table; Data Repository item 2017xxx.
[1]GSA Data Repository item 2016354, full field and laboratory sampling methods, sample locations, river basin data, beryllium isotope data, erosion rate data, and Hybla Valley core beryllium data, is available at http://www.geosociety.org/pubs/ft2016.htm or by request to editing@geosociety.org.
SCIENCE EDITOR: BRADLEY S. SINGER
ASSOCIATE EDITOR: JOEL PEDERSON
MANUSCRIPT RECEIVED _ MONTH 2016
REVISED MANUSCRIPT RECEIVED _ MONTH 2016
MANUSCRIPT ACCEPTED _ MONTH 2016
Printed in the USA

Erosion rates and sediment flux within the Potomac River basin quantified over millennial timescales using beryllium isotopes

Eric W. Portenga[1,†], Paul R. Bierman[2], Charles D. Trodick Jr.[3], Sophie E. Greene[3], Benjamin D. DeJong[2,§], Dylan H. Rood[4], and Milan J. Pavich[5]
[1]Department of Geography and Geology, Eastern Michigan University, Ypsilanti, Michigan 48197, USA
[2]Geology Department and Rubenstein School of the Environment and Natural Resources, University of Vermont, Burlington, Vermont 05405, USA
[3]Geology Department, University of Vermont, Burlington, Vermont 05405, USA
[4]Department of Earth Science and Engineering, Imperial College London, South Kensington Campus, London, SW7 2AZ, UK and *Center for Accelerator Mass Spectrometry, Lawrence Livermore National Laboratory, Livermore, California 94550, USA*
[5]Consulting Geologist, Rockland, Maine 04841, USA

ABSTRACT

Beryllium isotopes measured in detrital river sediment are often used to estimate rates of landscape change at a basin scale, but results from different beryllium isotope systems have rarely been compared. Here, we report measurements of *in situ* and meteoric ^{10}Be ($^{10}Be_i$ and $^{10}Be_m$, respectively) along with measurements of reactive and mineral phases of ^{9}Be ($^{9}Be_{reac}$ and $^{9}Be_{min}$, respectively) to infer long-term rates of landscape change in the Potomac River basin, North America. Using these data, we compare directly results from the two different ^{10}Be isotope systems and contextualize modern sediment flux from the Potomac River basin to Chesapeake Bay.

Sixty-two measurements of $^{10}Be_i$ in river sand show that the Potomac River basin is eroding on average at 29.6 ± 14.1 Mg km^{-2} yr^{-1} (11 ± 5.2 m m.y.$^{-1}$ assuming a rock density of 2,700 kg m^{-3}) – a rate consistent with other estimates in the mid-Atlantic region. $^{10}Be_i$ erosion rates correlate with basin latitude, suggesting that periglacial weathering increased with proximity to the former Laurentide Ice Sheet margin. Considering the $^{10}Be_i$-derived erosion rate as a sediment flux over millennia, rates of sediment delivery from the Potomac River to

Chesapeake Bay are ~10x lower than contemporary sediment yields implying modern land-use practices have accelerated erosion and sediment transport over background rates. However, $^{10}Be_i$ erosion rate data suggest that regulatory benchmark levels used to manage sediment export from the Potomac River basin to Chesapeake Bay are set appropriately to reduce sedimentation and restore the Bay's ecological health.

The mean of 56 $^{10}Be_m/^9Be_{reac}$-derived denudation rates (40.0 ± 21.7 Mg km^{-2} yr^{-1}) is higher than, but statistically indistinguishable from, the mean $^{10}Be_i$ erosion rate (29.6 ± 14.1 Mg km^{-2} yr^{-1}; $p = 0.003$). However, when considered basin by basin, $^{10}Be_m/^9Be_{reac}$ -determined denudation rates are only weakly correlated ($R^2=0.208$; $p < 0.001$) with sediment fluxes determined from the well-established and widely used $^{10}Be_i$ technique. This suggests that the $^{10}Be_m/^9Be_{reac}$ technique may not reflect the same geomorphic processes as $^{10}Be_i$ technique, or that the $^{10}Be_m/^9Be_{reac}$ technique operates over different time and/or depth scales. Erosion indices (EIs, *sensu* Brown et al., 1988) derived from $^{10}Be_m$ measurements and contemporary sediment yield data range from 0.07 to 1.24; 75% of basins sampled have EIs that are similar to or greater than 1, suggesting that $^{10}Be_m$ is being retained and sediment is being stored within the Potomac River basin. The Appalachian Plateau is the only physiographic province where sediment export dominates, likely as the result of on-going relief growth in catchments draining the Appalachian Mountain divide. $^{10}Be_m$ concentrations measured in the 150 k.y. Hybla Valley sediment core, taken from the lower Potomac River basin, suggest that $^{10}Be_m$ and sediment is preferentially stored in the catchment when vegetation proxies for climate change suggest warmer conditions prevail. $^{10}Be_m$ and sediment are exported when vegetation proxies for climate suggest conditions are colder, perhaps a reflection of periglacial activity or changes in storm frequency and/or magnitude over glacial/interglacial cycles.

INTRODUCTION

Understanding the effects that human land-use practices have on landscapes requires knowledge of background (geological) rates of sediment erosion and denudation, transport, and deposition (Hooke et al., 2012; Pelletier et al., 2015). Despite several decades of intensive data collection (Judson, 1968; McLennan, 1993; Milliman and Syvitski, 1992; Portenga and Bierman, 2011), there remain many landscapes for which there is little quantitative information about natural or background rates of landscape change (e.g., Arkle et al., 2017; Jonell et al., 2016; Mandal et al., 2015; Reusser et al., 2015, Struth et al., 2017). The Potomac River basin along the United States' east coast is a landscape where large volumes of sediment deposition in Chesapeake Bay are known to have resulted from widespread erosion associated with intensive European-American land-use practices in the 1700–1800s (Fig. 1; Brush, 2009; Costa, 1975; Kirby, 2004; Saenger et al., 2008). However, the effect of this human-induced land-use change on erosion and sediment transport rates remains only loosely constrained because background rates and spatial patterns of pre-disturbance landscape change are largely unknown.

Since the 1980s, the use of isotopic tracers, specifically the cosmogenic isotope ^{10}Be, has greatly increased our knowledge of the rate at which Earth surface processes operate (e.g., Graly et al., 2010; Harel et al., 2016; Portenga and Bierman, 2011; Willenbring and von Blanckenburg, 2010). Both the ^{10}Be produced by cosmic-ray interactions in the atmosphere (meteoric, $^{10}Be_m$) and that created by interactions in mineral grains at Earth's surface (*in situ*, $^{10}Be_i$) have been measured and used to infer process rates and trace sediment across the landscape (e.g., Brown et al., 1998; Helz and Valette-Silver, 1992; Kirchner et al., 2001; Ouimet et al., 2009; Portenga et al., 2017; Reusser and Bierman, 2010; Schaller et al., 2001; You et al., 1988). Recently, the stable isotope of beryllium, ^{9}Be, has been measured in soil and sediment, and its abundance has been used to normalize measured activities of ^{10}Be$_m$ produced in the atmosphere and incorporated in soil and sediment grain coatings (Dannhaus et al., 2018; Rahaman et al., 2017; von Blanckenburg et al., 2012; Wittmann et al., 2015). This ^{9}Be normalization approach was developed, in part, for the purpose of calculating denudation rates (total mass loss per unit area over time) at the basin scale in areas where quartz was not available for the now well-established ^{10}Be$_i$ erosion rate technique (Dannhaus et al., 2018; von Blanckenburg et al., 2012), which in most settings gives values for erosion (the mass of sediment removed per unit area over time; Lal, 1991).

In this paper, we report measurements of ^{10}Be$_i$ and ^{10}Be$_m$ in conjunction with measurements of reactive ^{9}Be (^{9}Be$_{reac}$, in this case, acid-extractable) coating sediment grains and unweathered ^{9}Be (^{9}Be$_{min}$) contained within the mineral grains of bulk sediment. We use the ^{10}Be$_i$ data to investigate spatial and temporal patterns of erosion, and by inference sediment flux, in the Potomac River basin in order to gain an understanding of the rates at which mass was delivered to Chesapeake Bay prior to the impacts of European-Americans settling the region. Together, these data allow us to compare rates of landscape change (erosion and denudation) calculated from ^{10}Be$_i$ and ^{10}Be$_m$/^{9}Be$_{reac}$ ratios (cf. von Blanckenburg et al., 2012) measured in the same samples. Contemporary sediment yield data are available for ten basins in the Potomac River watershed (Gellis et al., 2004); we compare these data to long-term erosion rates inferred from ^{10}Be$_i$. We also employ the method developed and tested by Brown et al. (1988) using ^{10}Be$_m$ to calculate erosion indices (EIs) for ten basins draining different physiographic provinces within the watershed. This method assesses the isotopic balance between ^{10}Be$_m$ entering and leaving a basin; because ^{10}Be$_m$ is adhered to sediment grain coatings, the EI serves as a proxy for the amount of sediment being retained within or exported from a basin. To provide a long-term context for the contemporary isotopic data, we also measured ^{10}Be$_m$ in 13 samples spanning the last 150 k.y., isolated from a sediment core collected in Hybla Valley, an abandoned meander of the lower Potomac River (Litwin et al., 2013).

In addition to providing specific information about the Potomac River basin, our data provide the first independent large-scale comparison between the two different ^{10}Be isotopic systems used to understand rates of basin-scale landscape change from detrital, fluvial sediment. We use the entire data set to address a variety of outstanding questions: How well-correlated are long-term denudation rates estimated using ^{10}Be$_m$/^{9}Be$_{reac}$ and erosion rates quantified using ^{10}Be$_i$? Are contemporary, short-term sediment yields similar to or different from long-term rates of landscape change inferred from Be isotopes? What roles do topography, landscape physiography, and human land use play in changing the landscape of the Potomac River basin?

Field Area

The Potomac River drains ~38,000 km^2 of the central Appalachian Mountains and is a major source of sediment to Chesapeake Bay, the largest estuary in the United States (Gellis et al., 2004; Fig. 1). Despite the importance of the Bay and its ecosystems to the ecology and economy of the mid-Atlantic region, little is known about the long-term rates of sediment export from the Potomac River basin to the Bay. Erosion rates of summit ridgelines throughout the central Appalachian Mountains, inferred from measured concentrations of ^{10}Be$_i$ in bedrock outcrops, are on the order of ~10 m m.y.$^{-1}$ (Duxbury et al., 2015; Hancock et al., 2015; Portenga et al., 2013). However, outcrops exist on ridgelines because they erode more slowly than the drainage basins they divide; inferring erosion rates or sediment generation rates over large areas (drainage basin scale) from outcrop data alone is not reasonable because of this bias.

Sediment in the Potomac River basin is derived from five physiographic provinces (Fig. 2). These provinces are delineated by significant changes in bedrock lithology, structural features, and topography. From west to east across the Potomac River basin, the physiographic provinces include: (1) the Appalachian Plateau, the western, mostly undeformed part of the foreland, which is underlain by Upper Paleozoic clastic and carbonate rocks; (2) the Valley and Ridge Province, which consists of Lower Paleozoic clastic and carbonate rock in the eastern, deformed part of the foreland, where they are folded into elongate synclines and anticlines; (3) the Blue Ridge, which is a mix of quartzite and volcanic rocks, widely recognized for providing the steep topography that makes up Shenandoah National Park; (4) the Piedmont region, which consists of rolling hills covered by mature soils and which is underlain by deeply weathered and heavily deformed Proterozoic gneiss (which formed the core of the Alleghenian orogeny); and (5) the Coastal Plain, which sits east of the Fall Line and consists mostly of Cretaceous and younger reworked fluvial, estuarine, and nearshore and marine sediments. Quartz-bearing rocks underlie all of these provinces.

Although the Potomac River basin was never glaciated, extensive periglacial weathering occurred at high elevations throughout the central Appalachians and is thought to have increased the amount of unconsolidated material available for delivery to offshore basins (Clark and Ciolkosz, 1988; Denn et al., 2018; Poag and Sevon, 1989; Whittecar and Ryter, 1992). Additionally, long-term flexural hydro-isostatic uplift of the land surface in and near the Potomac basin, which was the result of continued offshore sediment loading (Pazzaglia and Gardner, 1994), punctuated by higher-frequency glacial-isostatic adjustments (DeJong et al., 2015; Peltier, 1996), drove complex histories of land surface change and possibly caused higher rates of river incision near the Fall Line at Great Falls during times in the past (Bierman, 2015; Reusser et al., 2004).

Widespread land-use change in the Chesapeake Bay watershed began in the 1700s when European colonists, drawn by the fertile soils of the Appalachian Piedmont region and the vast oyster stocks in the Bay, moved into the region (Brown et al., 1988; Brush, 2009; Colman and Bratton, 2003; Cooper and Brush, 1993; Costa, 1975; Gellis et al., 2004; Kirby, 2004; Langland and Cronin, 2003; Montgomery, 2007; Saenger et al., 2008; Wolman, 1967). Up to 80% of land within the Chesapeake Bay watershed was deforested and used for agriculture by the late 1800s, which caused rapid erosion and delivery of topsoil, nutrients, and charcoal to the Bay at levels much higher than natural background (Brush, 2009; Cooper and Brush, 1993; Valette-Silver et al., 1986).

Only a few low dams have been constructed across the Potomac River (Gerhart, 1991), and therefore most of Potomac River's bedload is transported directly to Chesapeake Bay; however, milldams on small Potomac River tributaries effectively trapped sediment eroded after deforestation by European settlers (Walter and Merritts, 2008). These milldams have fallen into disrepair, and once-trapped sediment is now being released into the larger Potomac River basin. For the period of 1952–2001, the Potomac River was the largest contributor of sediment to the Bay, supplying ~44% of the total sediment flux (Gellis et al., 2004); this amount exceeds sediment yields from the larger, previously glaciated Susquehanna River basin to the north (Ives, 1978). However, Susquehanna River is heavily dammed, which likely leads to sediment retention and decreases sediment transport to the Bay, except during large floods, when sediment is scoured from the beds of reservoirs and transported downstream (Langland and Cronin, 2003; Langland and Hainly, 1997).

Human impacts since the 1700s and continuing until today have been particularly severe in and near the heavily populated urban areas of Baltimore and Washington, DC, where development has disturbed much of the land and increased sediment delivery to Chesapeake Bay (Brush, 2009; Dauer et al., 2000; Gellis et al., 2017; Wolman, 1967). Restoration of the Bay's ecological health depends, in part, on reducing sediment delivery from tributary rivers to pre-disturbance levels (Hassett et al., 2005; Langland and Cronin, 2003). Doing so requires knowledge of the spatial patterns and background rates of erosion and denudation in landscapes upstream from the Bay. This is a motivation for our study.

Isotopic Tracers

Cosmogenic ^{10}Be is produced as cosmic rays interact with O and N atoms both in rock and sediment at Earth's surface ($^{10}Be_i$, Lal and Peters, 1962) and in the atmosphere ($^{10}Be_m$; Brown, 1988). $^{10}Be_m$ subsequently falls to Earth's surface with precipitation or as dry fallout and then adheres to the surfaces of mineral grains in soil and sediment profiles, where it is incorporated into pedogenic grain coatings (Brown et al., 1981; Dixon et al., 2017; Graly et al., 2010; Pavich et al., 1985; Willenbring and von Blanckenburg, 2010). In this study, we measured isotopic concentrations of $^{10}Be_i$ and $^{10}Be_m$ in sand-sized detrital fluvial sediment, using the data as indicators of sediment sourcing, rates of landscape change, and spatial patterns of landscape behavior.

The isotope $^{10}Be_i$ is produced in the mineral lattices of rock and sediment at Earth's surface, and measuring its abundance in quartz has become widely accepted as a way of deriving long-term erosion rates of rock outcrops and drainage basins, as well as rates of soil formation (e.g., Bierman and Steig, 1996; Brown et al., 1995; Granger et al., 1996; Heimsath et al., 2006; Nishiizumi et al., 1986; and numerous other papers as summarized in Harel et al., 2016; Portenga and Bierman, 2011; Willenbring et al., 2013). After being produced in rock and soil on slopes, the regolith and the $^{10}Be_i$ that it contains are then eroded. This eroded sediment is eventually delivered to rivers, where it is mixed such that $^{10}Be_i$ concentrations measured in alluvium collected at any point along a stream can be used to derive a long-term erosion rate that averages over the upstream contributing area. The duration over which erosion is integrated is determined by the time it takes to erode through one cosmic-ray attenuation depth, ~60 cm of rock, and thus isotope concentration is inversely related to landscape stability (Lal, 1991) and biased toward the surface and recent erosion history. In slowly eroding, areas, such as the Appalachian Mountains, which occupy much of the Potomac River basin, $^{10}Be_i$ erosion rates integrate over 10^4 to 10^5 yr (e.g., Duxbury et al., 2015; Hancock and Kirwan, 2007; Linari et al., 2016; Matmon et al., 2003; Portenga et al., 2013; Reusser et al., 2015).

Slow erosion rates allow time for $^{10}Be_m$ to accumulate and be retained on sediment grain coatings during pedogenesis and before regolith is eroded and transported (Barg et al., 1997; Greene, 2016; Wittmann et al., 2015). If grain coatings are stable and there is negligible loss of $^{10}Be_m$ from soils in the dissolved phase, then concentrations of $^{10}Be_m$ would be correlated with concentrations of $^{10}Be_i$ in sediment and thus anticorrelated with $^{10}Be_i$ erosion rates and other metrics of $^{10}Be_i$-derived sediment fluxes. Such relationships have been observed in the whole of the Amazon River basin (von Blanckenburg et al., 2012). The isotope $^{10}Be_m$ has also been used as a sediment tracer in a variety of fluvial systems (Brown et al., 1988; Helz and Valette-Silver, 1992; Portenga et al., 2017; Reusser and Bierman, 2010; Valette-Silver et al., 1986; van Geen et al., 1999). However, identifying sediment sources in basins as large as the Potomac River basin is challenging.

Questions about $^{10}Be_m$ stability after incorporation into sediment grain coatings, and thus geomorphological interpretations based on measurements of $^{10}Be_m$ concentration in these coatings, have motivated the search for a method to normalize $^{10}Be_m$ concentrations using another isotope with similar chemical behavior (Bacon et al., 2012; Wittmann et al., 2012, 2015). Once regolith is eroded from rock outcrops and subcrops, most native ^{9}Be ($^{9}Be_{parent}$) remains within silicate mineral crystal lattices ($^{9}Be_{min}$); however, chemical weathering releases some ^{9}Be to soil solutions and groundwater (von Blanckenburg et al., 2012). The ^{9}Be that is incorporated into sediment grain coatings is termed the reactive phase ($^{9}Be_{reac}$), and the dissolved portion is termed the dissolved phase ($^{9}Be_{diss}$; von Blanckenburg et al., 2012, Wittmann et al., 2015). ^{9}Be is thought to adhere to mineral grains via the same mechanisms as $^{10}Be_m$ (Barg et al., 1997; von Blanckenburg et al., 2012); thus, the $^{10}Be_m/^{9}Be_{reac}$ ratio is assumed to be locked at the time of coating deposition and can be considered a closed system (Graly et al., 2010). Based on this closed-system model, the $^{10}Be_m/^{9}Be_{reac}$ ratio of authigenic minerals or sediment grain coatings has been proposed as an independent measure of rates of landscape change (von Blanckenburg et al., 2012). In the laboratory, this weathering-sourced $^{9}Be_{reac}$ can be removed from sediment grains using a variety of methods that have been shown to remove little, if any, mineral lattice ^{9}Be (i.e., $^{9}Be_{min}$) incorporated in silicate minerals (Greene, 2016; Wittmann et al., 2012).

Erosion and denudation are often confused and/or equated but their definitions are important and distinct in the context of ^{10}Be production and/or delivery and retention on landscapes. Here, we define erosion measured using $^{10}Be_i$ as the mass of solid material lost from an area of Earth's surface over time (a rate, $M\ L^{-2}\ T^{-1}$). Assuming a density ($M\ L^{-3}$), erosion can be reported in units of $L\ T^{-1}$. Erosion rates, as described below, can be derived from both $^{10}Be_i$ and $^{10}Be_m$ and, assuming steady state, one can equate the mass of physical material supplied by erosion over time to the sediment flux out of a basin; in other words, all eroded sediment ends up in the river eventually with no net change in long-term sediment storage. In contrast, denudation is the total physical and chemical mass lost per unit area over a given duration of time, again in units of $M\ L^{-2}\ T^{-1}$. In this study, denudation rates are inferred from $^{10}Be_m/^{9}Be_{reac}$ ratios. By definition, denudation includes both erosion and mass lost by dissolution and therefore denudation rates cannot be lower than erosion rates or inferred long-term sediment fluxes.

Depending on the geomorphic setting, $^{10}Be_m$ and $^{10}Be_i$ may integrate mass loss rates over different depths. $^{10}Be_i$ is most sensitive to physical mass loss in the uppermost few meters of the soil/regolith system – the depth of $^{10}Be_i$ production through fast neutron penetration and spallation. In contrast, the $^{10}Be_m$ system begins recording information about the cumulative physical and dissolved mass loss at the weathering front, which in some settings can be much deeper than the penetration depth of most cosmic rays. For example, in the Potomac River basin, the weathering front is within the cosmic ray penetration depth over much of the Appalachian Plateau, Valley and Ridge, and the Blue Ridge, where soils are shallow on steep hillslopes. However, in the Piedmont, meters of saprolite can overly the weathering front (Pavich, 1989, 1990); thus, mass in the Piedmont is lost by solution below the penetration depth of most cosmic rays. As a result of mass loss by solution below the penetration depth of cosmic rays, there exists the possibility that quartz grains remaining in soil profiles reside on the landscape longer than the residence time of bulk, non-quartz material (Riebe et al., 2001). In this case, measurements of $^{10}Be_i$ result in erosion rates that are less than the rate of total denudation, as recorded by the $^{10}Be_m$ system, because $^{10}Be_i$ does not directly track mass loss by solution at depth. Such thinking is not relevant to the Coastal Plain, which is made up predominantly of reworked quartz-rich sand and gravel with few primary minerals left to weather. It is important, therefore, to make the distinction between $^{10}Be_i$ erosion rates, which refer primarily to the physical mass loss from landscapes within the $^{10}Be_i$ nuclide production depth and $^{10}Be_m/^{9}Be_{reac}$ denudation rates, which model total mass loss from the entire depth of regolith.

METHODS

We collected stream sediment from 70 sub-basins within the Potomac River watershed (Fig. 2; Table DR1[1]) for analysis of $^{10}Be_i$, $^{10}Be_m$, $^{9}Be_{reac}$, and $^{9}Be_{min}$. Of these, 10 samples were collected at locations with present or former U.S. Geological Survey (USGS) gauging stations and associated documented long-term annual sediment yields (Gellis et al., 2004). Most samples were collected from small basins (5–100 km^2) in each of the five physiographic provinces drained by Potomac River. During sample collection, we observed minimal signs of major human disturbance that could potentially serve as a point source for deeply sourced or recently excavated sediment, which would therefore not be indicative of long-term background surface erosion rates (e.g., gravel pits, quarrying; Fig. 2). Sampled basins were small enough to be occupied by one primary land use: forested, agricultural, or urban (classifications derived from a national land cover database, accessed on 21 July 2011; NOAA, 2010).

Alluvium was collected from streambeds or point bars and sieved in the field to the 250–850 µm grain-size fraction for both $^{10}Be_i$ and $^{10}Be_m$ analyses. Several studies have shown that the concentration of $^{10}Be_m$ can be higher on smaller grain sizes than on coarser material (Dannhaus et al., 2018; Pavich et al., 1985; Singleton et al., 2015), which could lead to biases in determinations of the denudation rate (von Blanckenburg et al., 2012); however, $^{10}Be_m$ grain-size dependencies are minimized when $^{10}Be_m$ is normalized to $^{9}Be_{reac}$ (Singleton et al., 2015; von Blanckenburg et al., 2012; Wittmann et al., 2012). Samples from each basin were used for $^{10}Be_m$ analyses (n = 70); sufficient amounts of pure quartz were extracted from samples for the majority of basins (n = 62), from which $^{10}Be_i$ was used to calculate basin-averaged, long-term erosion rates (Bierman and Steig, 1996; Brown et al., 1995; Granger et al., 1996).

The ^{10}Be samples were prepared for isotope dilution chemistry using a ^{9}Be carrier solution that was added during sample processing. Beryllium was isolated and purified using the methods of Corbett et al. (2016) for $^{10}Be_i$ and Stone (1998) for $^{10}Be_m$ samples. Beryllium isotope ratios ($^{10}Be/^{9}Be$) were measured by accelerator mass spectrometry (AMS) at the Lawrence Livermore National Laboratory (Rood et al., 2010), blank-corrected, and normalized to the 07KNSTD standard assuming a standard ratio of 2.85×10^{-12} (Nishiizumi et al., 2007; Table DR2). We summarized $^{10}Be_i$ production across each sampled basin to a single point in space and calculated basin-scale erosion rates from $^{10}Be_i$ data using the CRONUS online calculator (Balco et al., 2008; main calculator, version 2.1) using a global $^{10}Be_i$ production rate and scaling schemes of Lal (1991) and Stone (2000). Typically, cosmogenic erosion rates are representative of all upstream catchment areas contributing sediment to that sample, but here we present erosion rates that reflect the un-overlapped portions of nested catchments following Granger et al. (1996); we refer to these erosion rates as unnested erosion rates, and we use the unnested rates for all following calculations and statistics (Table DR3).

In addition to $^{10}Be_i$ erosion rates, deriving erosion rates from single measurements of $^{10}Be_m$ has previously been proposed (Brown et al., 1988), but the idea was supplanted by the more straightforward $^{10}Be_i$ erosion rate technique described above. Recently, however, deriving erosion rates from $^{10}Be_m$ has been revisited (von Blanckenburg et al., 2012; Willenbring and von Blanckenburg et al., 2010) using the following equation:

$$E = \frac{^{10Be}F_{met}}{[^{10}Be_m]}, \quad (1)$$

Here, $^{10Be}F_{met}$ is the $^{10}Be_m$ delivery rate (atoms cm^{-2} yr^{-1}) and [$^{10}Be_m$] is the concentration of $^{10}Be_m$ (atoms g^{-1}). E, the erosion rate, is expressed in units of g cm^{-2} yr^{-1}; however, we convert these units and present E in units of Mg km^{-2} yr^{-1}. E is also commonly expressed in units of m m.y.$^{-1}$ by taking the quotient of E and bulk rock density (e.g. 2.7 g cm^{-3}), then converting units.

Denudation rates, total mass loss from both chemical and physical processes, can also be derived using $^{10}Be_m$ by normalizing $^{10}Be_m$ measurements to $^{9}Be_{reac}$ measurements, using a rearrangement of von Blanckenburg et al.'s (2012) mass-balanced Equation 12:

$$D = \frac{^{10Be}F_{met} \times \left(\frac{[^9Be]_{min}}{[^9Be]_{reac}} + 1\right)}{[^9Be]_{parent} \times \left(\frac{^{10}Be_m}{^{9}Be_{reac}}\right)}, \quad (2)$$

where D is the denudation rate (g cm^{-2} yr^{-1}), and $[^9Be]_{parent}$, $[^9Be]_{min}$, and $[^9Be]_{reac}$ are the native, mineral, and reactive concentrations of ^{9}Be, respectively (atoms g^{-1}). Here, we convert units and present D in units of Mg km^{-2} yr^{-1}. Importantly, Equation 2 assumes that there is minimal mass flux of ^{9}Be dissolved in stream water, an assumption that is likely valid considering that average pH measurements from nine of the ten sampled streams with USGS gauging stations (Fig. 2) are between 7.0–8.1 (average measurement period: 30 yrs; average number of pH measurements per station: 270; no pH data were available for the tenth gauging station, 01650500). In contrast, pH < 4 is typically required to strip all Be from grain coatings (Åström et al., 2018; Graly et al., 2010; Willenbring et al., 2010). Data for these nine USGS gauging stations were accessed through the USGS National Water Information System (https://maps.waterdata.usgs.gov/mapper). Because there are likely negligible amounts of $^9Be_{parent}$ being lost in the dissolved phase, $^{10}Be_m/^9Be_{reac}$ denudation rates can be directly compared to $^{10}Be_i$ erosion rates assuming that soil depths are similar to or less than the depth of cosmic ray penetration (Pavich, 1989, 1990). If the weathering front is deeper than a few meters, $^{10}Be_m/^9Be_{reac}$ denudation rates should exceed $^{10}Be_i$ erosion rates.

von Blanckenburg et al.'s (2012) mass-balance approach, and thus Equation 2 can only be used if certain criteria are met: (1) $^{10Be}F_{met}$ is known or can be reasonably estimated, (2) $[^9Be]_{parent}$ is known or can be assumed, (3) the $^{10}Be_m/^9Be_{reac}$ ratio has achieved equilibrium in the weathering zone, (4) the $^{10}Be_m/^9Be_{reac}$ ratio of beryllium adhered to sediment is in equilibrium with the $^{10}Be_m/^9Be_{reac}$ ratio of beryllium dissolved in a river basin, (5) the basin area is of sufficient size to average out natural variations of the $^{10}Be_m/^9Be_{reac}$ ratios, (6) radioactive decay of $^{10}Be_m$ is negligible, (7) $^{10}Be_m$ and $^9Be_{reac}$ can be extracted from sediment, and (8) the fractional flux of ^{9}Be released from bedrock parent material, von Blanckenburg et al's (2012) ($^{9Be}f_{reac}$ + $^{9Be}f_{diss}$) term, is known.

Information presented below suggest that each of the criteria listed above are reasonably met in the Potomac River basin. (1) The $^{10}Be_m$ flux rate we use, $^{10Be}F_{met}$ (atoms cm^{-2} yr^{-1}), is derived from observed relationships among measured deposition rates, precipitation rate (P, in cm yr^{-1}), and latitude (L) (Graly et al., 2011) such that:

$$^{10Be}F_{met} = P \times \frac{1.44}{\left(1 + e^{\left(\frac{(30.7 - L)}{4.36}\right)}\right) + 0.63}. \quad (3)$$

Values of $^{10Be}F_{met}$ for individual catchments range from 1.5–2.5 x 10^6 atoms cm^{-2} yr^{-1}, with an average of 2.0 x 10^6 atoms cm^{-2} yr^{-1}, which is consistent with an average Holocene $^{10Be}F_{met}$-value of 2.0 x 10^6 atoms g^{-1} yr^{-1} (Heikkilä and von Blanckenburg, 2015). (2) We did not directly measure $[^9Be]_{parent}$, and we follow von Blanckenburg et al. (2012) in assuming an average crustal $[^9Be]_{parent}$ concentration of 2.5 ppm. (3) The catchments that our samples come from are long-established and we thus assume that the $^{10}Be_m/^9Be_{reac}$ ratio has equilibrated in the weathering zone. (4) There is minimal dissolved beryllium considering regional river water pH values at stream gauging stations and thus the $^{10}Be_m/^9Be_{reac}$ ratios are fully equilibrated between reactive

DOI:10.1130/B31xxx.1

and dissolved phases. (5) The measured catchments are sufficiently large (5–30,000 km^2) to ensure sediment mixing. (6) Little $^{10}Be_m$ has decayed between its production and sample collection because rates of erosion limit regolith residence time on the landscape to much less than the half-life of ^{10}Be. (7) The HCl leaching technique removes primarily $^{10}Be_m$ and $^{9}Be_{reac}$ from sediment grain coatings and leaches little if any $^{9}Be_{min}$ (Greene, 2016) as indicated by minimal Si in the leachate. (8) The ($^{9Be}f_{reac}$ + $^{9Be}f_{diss}$) term is implicit in Equation 2 (above) by the following rearrangements of von Blanckenburg et al.'s (2012) Equations 9 and 10, respectively:

$$\left({}^{9Be}f_{reac} + {}^{9Be}f_{diss}\right) = \frac{{}^{10Be}F_{met}}{D \times [{}^{9}Be]_{parent} \times \left(\frac{{}^{10}Be_m}{{}^{9}Be_{reac}}\right)}, \qquad (4)$$

and

$$\frac{1}{\left(\frac{[{}^{9}Be_{min}]}{[{}^{9}Be_{reac}]} + 1\right)} = \frac{{}^{10Be}F_{met}}{D \times [{}^{9}Be]_{parent} \times \left(\frac{{}^{10}Be_m}{{}^{9}Be_{reac}}\right)}. \qquad (5)$$

The right-hand sides of Equations 4 and 5 are equal; therefore:

$$\left({}^{9Be}f_{reac} + {}^{9Be}f_{diss}\right) = \frac{1}{\left(\frac{[{}^{9}Be]_{min}}{[{}^{9}Be]_{reac}} + 1\right)}. \qquad (6)$$

Importantly, Equations 4–6 (above) assume there is negligible ^{9}Be leaving any catchment in the dissolved phase, which reduces the denominator in von Blanckenburg et al.'s (2012) Equation 10 to unity. Note that Equation 5 (above) is also a rearrangement of von Blanckenburg et al.'s (2012) Equation 12, which we rearranged to solve for *D* in Equation 2 of this paper.

Erosion indices (EIs), calculated only for samples for which there is annual sediment load data (n = 10, Gellis et al., 2004) were quantified using the approach of Brown et al. (1988):

$$EI = \frac{M \times [{}^{10}Be_m]}{A \times {}^{10Be}F_{met}}, \qquad (7)$$

where M is the annual sediment load (g yr^{-1}), [$^{10}Be_m$] is the isotopic concentration of $^{10}Be_m$ (atoms g^{-1}), and A is river basin area (cm^2). EIs are <1 when more $^{10}Be_m$ is delivered to the basin by precipitation than is exported in sediment grain coatings; consequently, ^{10}Be, and sediment by inference, is stored within the river basin. Conversely, EIs >1 indicate rates of $^{10}Be_m$ export exceed rates of $^{10}Be_m$ delivery to a basin, and this can be used to infer sediment export.

All $^{10}Be_m$, ^{9}Bereac, and $^{9}Be_{min}$ samples were processed at the University of Vermont Cosmogenic Nuclide Laboratory (Table DR2; www.uvm.edu/~cosmolab). The $^{9}Be_{reac}$ was measured on aliquots of all samples (n = 70) by inductively coupled plasma–optical emission spectrometry (ICP-OES) after being leached using heated, ultrasonic etching in 6 M HCl (Greene, 2016). The $^{9}Be_{min}$ was extracted from already acid-etched bulk sediment from 57 of the 70 basins by a multistep open-beaker hotplate procedure using concentrated H_2O_2, HNO_3, HF, and $HClO_4$ (see data repository for detailed sample processing procedures [see footnote 1]). ICP-OES measurements of Si in the 6 M HCl leachate, extracted at different time intervals during the leaching process, indicate that predominately $^{9}Be_{reac}$ in grain coatings was removed and $^{9}Be_{min}$ in primary silicate minerals was left intact (Greene, 2016).

Brown et al. (1988) compared the flux of $^{10}Be_m$ entering drainage basins via precipitation with that adhered to sediment (as grain coatings) exiting the same basins in order to assess where sediment export or storage occurs throughout the Appalachian Mountains; they termed this ratio the erosion index (EI) and made their measurements in bulk sediment samples after testing for and finding little effect of grain size on $^{10}Be_m$ concentration in one sample. Three of Brown et al.'s (1988) sampled basins are located within the Potomac River basin. Brown et al. (1988) found that, in general, EIs were very sensitive to land-use practices and that catchments draining the Piedmont region along the entire US east coast were exporting rather than storing sediment.

We recalculated Brown et al.'s (1988) EI values for sub-basins in the Potomac River basin using more than 20 yr of precipitation data (Hijmans et al., 2005) and basin-specific $^{10}Be_m$ delivery estimates (Eq. 3; Graly et al., 2011). We adjusted Brown et al.'s (1988) published $^{10}Be_m$ concentrations by a factor of 0.9042 (see hess.ess.washington.edu/math/docs/al_be_v22/al_be_docs.html) because the reported concentrations were originally derived using the ICN/KNSTD AMS standard material, which was the primary standard material used at University of Pennsylvania at the time Brown made his measurements (Middleton et al., 1993; Nishiizumi et al., 2007); the correction factor is based on an updated ^{10}Be AMS standard value, which is consistent with a change in the accepted ^{10}Be half-life (Nishiizumi et al., 2007).

To understand how the $^{10}Be_m$ concentration of sand-sized sediment moving through the Potomac River has changed over time (150 k.y.), we measured the concentrations of $^{10}Be_m$ adhered to sediment extracted from 13 samples from the well-dated Hybla Valley sediment core (Fig. 2; Litwin et al., 2013). A similar approach was used to infer histories of sediment delivery to Chesapeake and San Francisco Bays (Helz and Valette-Silver, 1992; Valette-Silver et al., 1986; van Geen et al., 1999).

RESULTS

Long-term, background $^{10}Be_i$-based erosion rates (Tables DR2 and DR3 [see footnote 1]) for 62 Potomac River basins range from 8 to 104 Mg km^{-2} yr^{-1} (3 to 39 m m.y.$^{-1}$) and are normally distributed according to a Shapiro-Wilk goodness-of-fit test ($p = 0.23$; Fig. 2). We used a Grubb's outlier test to identify statistical outliers, which we investigated further to determine if these samples were collected from severely disturbed basins. Although both samples POT20 and POT45 were identified as outliers, we only exclude POT20 from further analyses (including all $^{10}Be_m$-based analyses) because it drains a large portion of agricultural research land that is heavily disturbed and because there is no certainty that all sediment derived upstream of POT20 originated from within the basin, as some may have been brought in from elsewhere for research purposes. The mean $^{10}Be_i$ erosion rate for the Potomac River basin is 29.6 ± 14.1 Mg km^{-2} yr^{-1} (11.0 ± 5.2 m m.y.$^{-1}$; 1σ, $n = 61$), and median and area-weighted mean erosion rates are within the uncertainty of the mean. At these erosion rates, material resides within the uppermost ~60 cm of Earth's surface for ~55 k.y., on average, integrating over much of the last glacial-interglacial cycle. However, ten contemporary sediment yield measurements (Gellis et al., 2004) are up to ~10x greater than the background sediment flux calculated from $^{10}Be_i$ (Fig. 3a). Potomac River erosion rates derived from $^{10}Be_m$ using the two-factor Equation 1 are, in nearly every case, greater than $^{10}Be_i$ erosion rates (Fig. 3b). No systematic offset exists between the two erosion rate datasets, except in the Coastal Plain where $^{10}Be_m$ erosion rates are consistently ~20x greater than $^{10}Be_i$ erosion rates.

$^{10}Be_i$ erosion rates are correlated to mean basin slope in the Potomac River basin ($R^2 = 0.115$; $p = 0.008$); this correlation, while significant, is much weaker than the correlations between $^{10}Be_i$ erosion rates and slope found in other nonglaciated basins in the Appalachian Mountains: $R^2 = 0.54$ for the Blue Ridge Escarpment (Linari et al., 2016); $R^2 = 0.42$ for the Great Smoky Mountains (Matmon et al., 2003); $R^2 = 0.58$ for the Susquehanna River basin (Reuter, 2005). As a whole population, $^{10}Be_i$ erosion rates in the Potomac Basin ($n = 61$) are correlated with mean basin elevation ($R^2 = 0.160$; $p = 0.001$) and mean annual precipitation ($R^2 = 0.146$; $p = 0.002$; Hijmans et al., 2005), but not with basin relief ($R^2 = 0.034$; $p = 0.156$) or basin area ($R^2 = 0.022$; $p = 0.253$); $^{10}Be_i$ erosion rates exhibit a weak but significant correlation ($R^2 = 0.065$) – after rounding ($p = 0.047$) – with latitude, which is a proxy for distance from the

Last Glacial Maximum ice-sheet margin. All elevation data were derived from the 90 m Satellite Radar Topography Mission dataset, downloaded from earthexplorer.usgs.gov.

Analysis of variance of $^{10}Be_i$ erosion rates shows no distinguishable difference in the mean erosion rate of samples from different land-use categories (Fig. 4a). Similarly, analysis of variance of $^{10}Be_i$ erosion rates in the five physiographic provinces shows that there is no statistical difference in the mean $^{10}Be_i$ erosion rates from any province (Fig. 4b). We note, however that there is a wider range in erosion rates in the Appalachian Plateau and that the $^{10}Be_i$ rates from the Coastal Plain may be lower than those from other provinces since the *p*-value for this analysis is equal to the significance threshold after rounding ($p = 0.048$).

$^{10}Be_m$ concentrations and $^{10}Be_i$ concentrations are not correlated when considered as a whole population ($R^2 = 0.044$, $p = 0.104$; Fig. 3c). However, positive correlations between $^{10}Be_m$ and $^{10}Be_i$ concentrations are observed in the Appalachian Plateau ($R^2 = 0.664$, $p = 0.048$), Valley and Ridge ($R^2 = 0.277$, $p = 0.025$), and Coastal Plain ($R^2 = 0.981$, $p < 0.001$) physiographic provinces (Fig. 3c). $^{10}Be_m/^9Be_{reac}$ are not related within statistical significance to $^{10}Be_i$ erosion rates throughout the Potomac River basin (e.g., $p > 0.05$, Fig. 5). When considering all Potomac samples, denudation rates derived from $^{10}Be_m/^9Be_{reac}$ ratios using Equation 2 are weakly correlated to $^{10}Be_i$ erosion rates ($R^2 = 0.208$, $p < 0.001$; Fig. 3d; Table DR3 [see footnote 1]); a Students *t*-Test shows the means of these two datasets to be similar as well ($p = 0.003$). Although weakly correlated, $^{10}Be_i$ erosion rates for individual basins are not reproduced well by $^{10}Be_m/^9Be_{reac}$ denudation rates. We find that $^{10}Be_m$ erosion rates are often much greater than $^{10}Be_m/^9Be_{reac}$ denudation rates.

EIs for samples we collected and those from three sites of Brown et al. (1988) within the Potomac River watershed are representative of the total upstream $^{10}Be_m$ isotopic balance (Brown et al., 1988). EIs calculated for the same basins sampled ~20 yr apart by us and those reported in Brown et al. (1988) are nearly equivalent (e.g., EI = 0.55 for POT06 and EI = 0.58 for USGS gauging station 01638500) and thus are reproducible over time. EIs for samples POT01–POT13 range from 0.07 to 1.24, and the EIs of POT02, POT10, POT12 are within 10% of equilibrium with respect to $^{10}Be_m$ delivery and export (Fig. 6; Table DR3 [see footnote 1]). EIs for sample sites that drain large portions of the Valley and Ridge (e.g. POT01, POT06 and gauging station 01638500) or small portions of the Piedmont provinces (e.g. POT 04, POT05, POT09, POT13) are generally <1; basins draining large portions of the Piedmont (e.g. gauging station 01643000), small basins in the Valley and Ridge (e.g. gauging station 01610200), and the Appalachian Plateau (e.g. POT11) are all >1.

DISCUSSION

Our measurements of $^{10}Be_i$, $^{10}Be_m$, $^9Be_{min}$, and $^9Be_{reac}$ from the Potomac River basin allow us to determine the pace of landscape change ($^{10}Be_i$ erosion rates) and to revisit and evaluate three uses of $^{10}Be_m$ proposed by others (cf. Brown et al., 1988; von Blanckenburg et al, 2012; Willenbring and von Blanckenburg, 2010): as a metric of erosion ($^{10}Be_m$), as a metric of denudation ($^{10}Be_m/^9Be_{reac}$), and as a measure of landscape stability using the erosion index (sediment yield and $^{10}Be_m$). Our comparison between $^{10}Be_i$ and $^{10}Be_m$-derived erosion and denudation metrics is an important experiment to conduct because it independently tests and applies to a new geographic region the approach suggested by von Blanckenburg et al. (2012) and implemented thus far by Dannhaus et al. (2018), Rahaman et al. (2017), and Wittmann et al. (2015).

Comparison of $^{10}Be_i$, $^{10}Be_m$, and $^{10}Be_m/^9Be_{reac}$-inferred rates of landscape change

Interpreting $^{10}Be_m$ alone in measured in detrital, fluvial sediment as erosion rates using

DOI:10.1130/B31xxx.1

eq. 1 does not produce accurate erosion rate data; in most cases, $^{10}Be_m$ overestimates, sometimes grossly, erosion rates determined using $^{10}Be_i$. Although concentrations of $^{10}Be_m$ and $^{10}Be_i$ are correlated in Potomac River sediment collected from sub-basins in the Appalachian Plateau (n = 5), Valley and Ridge (n = 18), and Coastal Plain (n = 7), no such correlation exists in the Piedmont and the Blue Ridge provinces, nor over the Potomac Basin sample set as a whole. These data thus suggest that concentrations of $^{10}Be_m$ as we collected it (e.g. sand-only sized fraction) do not reliably represent regolith residence times. This conclusion is consistent with von Blanckenburg et al.'s (2012) advocacy of a more complex analytical approach involving the measurement of $^{10}Be_m/^{9}Be_{reac}$ and the incorporation of other assumed and measured parameters (eq. 2 and 6).

In contrast to the $^{10}Be_m$ system, average rates of landscape change measured using $^{10}Be_m$ $^{10}Be_m/^{9}Be_{reac}$ and $^{10}Be_i$ are more similar indicating that normalization by $^{9}Be_{reac}$ is important and reasonable. However, differences between the $^{10}Be_m/^{9}Be_{reac}$ and $^{10}Be_i$ systems remain and are are most apparent in data from the Piedmont province, which differs from the other physiographic provinces in the Potomac River basin because it has very thick regolith and thus great depth to the weathering front. Measurements of $^{10}Be_i$ will underestimate the total mass lost in such landscapes because of mass loss by solution and groundwater export at depths below most *in situ* nuclide production (e.g. Riebe et al., 2001). A maximum value for solution loss below the depth of cosmic ray penetration can be approximated by the dissolved load of streams at base flow; Pavich (1990) made such calculations for the Piedmont and suggests that 10.8 Mg km^{-2} yr^{-1} is lost in solution (~4 m m.y.$^{-1}$, assuming a density of 2,700 kg m^{3}). If all solutes in the Piedmont originate below the cosmic ray penetration depth, the discrepancy between $^{10}Be_i$ erosion rates and $^{10}Be_m/^{9}Be_{reac}$ denudation rates in the Piedmont (30.8 Mg km^{-2} yr^{-1} and 46.7 Mg km^{-2} yr^{-1}, respectively) can be, for the most part, resolved by adding the mass lost to solution (Pavich, 1990) to the $^{10}Be_i$ inferred erosion rate. This yields a total mass loss rate in the Piedmont (41.6 Mg km^{-2} yr^{-1}, dissolved load plus $^{10}Be_i$ inferred erosion rate), closer to the measured $^{10}Be_m/^{9}Be_{reac}$ denudation rate (46.7 Mg km^{-2} yr^{-1}).

The lack of consistent agreement, for almost all sub-basins, between the $^{10}Be_i$ and $^{10}Be_m$ erosion rates (Fig. 3b) and between $^{10}Be_i$ erosion rates and $^{10}Be_m/^{9}Be_{reac}$ denudation rates (Fig. 3d) suggests that $^{10}Be_m$ methods are not accurately measuring long term rates of landscape change at the sub-basin scale, at least in the Potomac River basin. Our observation that $^{10}Be_m/^{9}Be_{reac}$ denudation rates do not replicate $^{10}Be_i$ erosion rates in the Blue Ridge – the steepest of all sampled provinces, and thus the one with the thinnest soils – and that $^{10}Be_m$ erosion rates are generally much greater than $^{10}Be_m/^{9}Be_{reac}$ denudation rates throughout a landscape where soils are generally thin, suggests noise in the $^{10}Be_m$-based data sets exceeds that of the $^{10}Be_i$-based data sets.

Such noise is not surprising considering the complexity of $^{10}Be_m$ behavior in the near-surface weathering system where physical, chemical, biologic, and pedogenic processes control $^{10}Be_m$ distribution over time, depth and space (Graly et al., 2010). This stands in contrast to $^{10}Be_i$, for which the production function with depth and over space and time is well constrained by the relevant nuclear physics. Below, we speculate on what factors might lead to both scatter and bias in rates derived from $^{10}Be_m$ and $^{9}Be_{reac}$ data in contrast to $^{10}Be_i$.

Grain Size Bias

Measuring $^{10}Be_m$ and $^{9}Be_{reac}$ on sand-size sediment underestimates total $^{10}Be_m$ and $^{9}Be_{reac}$ because there is relationship between grain coating volume, surface area, and grain size (Graly et al., 2010; Wittmann et al., 2012). In theory (von Blanckenburg et al., 2012), the ratio between the two isotopes of Be should be constant and thus denudation rates inferred from $^{10}Be_m/^{9}Be_{reac}$ should be unaffected by grain size. This assertion has been independently investigated (Singleton et al., 2016) who found that while the normalizing $^{10}Be_m$ to $^{9}Be_{reac}$ does not completely correct for grain-size biases, the bias was greatly diminished (i.e. a ~1.7 to 6-fold difference between $^{10}Be_m$ on clays compared to medium sand when uncorrected, versus a ~1.2 to 3-fold difference between $^{10}Be_m$ on clays compared to medium sand). The issue of grain size is a difficult one. Although $^{10}Be_m$ and $^{9}Be_{reac}$ can be measured in different size fractions, such data are of limited utility unless one knows the grain-size specific mass flux from a basin. Data that as far as we know are unavailable except in unique circumstances such as where all sediment leaving a basin is trapped and analyzed for grain size abundance.

Although grain size is doubtless important for interpreting measured $^{10}Be_m$ concentrations, data suggest its effect in the Potomac basin is miniumal. First, most sediment transport occurs in the Potomac region during large storms at which time sand is the most common grain-size transported (Brown et al., 1988). Consistent with other studies using the $^{10}Be_m/^{9}Be_{reac}$ technique (e.g. Dannhaus et al., 2018; Rahaman et al., 2017; Wittmann et al., 2015) we sampled the most commonly transported grain size, in this case, sand. Second, Brown et al. (1988) only found 1% of total $^{10}Be_m$ was exported in the <250 μm grain-size fraction of an Appalachian stream similar to those we sampled. Third, in this study we normalized $^{10}Be_m$ using ^{9}Be measurements, which should have significantly reduced grain size biases (von Blanckenburg et al., 2012).

Sample Processing Bias

In extracting $^{10}Be_m$ and $^{9}Be_{reac}$ from sediment grain coatings, we pulverized the sediment and performed a 6 M HCl leach on each sample. Using a strong acid leach on pulverized sample material differs from other studies that leach original material using both 0.5 M HCl and hydroxylamine-hydrochloride solutions (Wittmann et al., 2012). Laboratory measurements of the solute taken from our samples at intervals during the etching process demonstrate that 6 M HCl did not remove any significant amount of Si. Silica in solution would be an indication that silicate minerals, including quartz, were dissolved to some degree, releasing $^{9}Be_{min}$ into solution; thus, we conclude little if any $^{9}Be_{min}$ was incorporated into the $^{9}Be_{reac}$ measurements (Greene, 2016; Singleton et al. 2016).

Unconstrained $^{9}Be_{parent}$ or $^{10Be}F_{met}$

We did not measure the amount of naturally-occurring $^{9}Be_{parent}$ in bedrock samples from all lithologies throughout the Potomac River basin and no such data are available. Rather, we follow previous studies in assuming a bulk crustal $^{9}Be_{parent}$ concentration (von Blanckenburg et al., 2012). Doing so introduces uncertainty into the value of the denominator in Equation 2.

It is possible that the $^{10}Be_m$ delivery rate ($^{10Be}F_{met}$) has changed through time. However, average Holocene $^{10Be}F_{met}$ rates (Heikkila and von Blanckenburg, 2015) are similar to the $^{10Be}F_{met}$ rates we calculated for our field area following Graly et al. (2011) which is based on contemporary $^{10}Be_m$ flux data. If our data sets are affected by inaccurate representations of $^{9}Be_{parent}$ or $^{10Be}F_{met}$, all samples would be affected, and the scatter in our data sets would be unchanged.

Effects of colonial-era land use in the Potomac Region

European-American colonial-era land use is the most likely and reasonable explanation for the disagreement between $^{10}Be_i$ and $^{10}Be_m$ erosion rates, between $^{10}Be_m$ erosion rates and $^{10}Be_m/^{9}Be_{reac}$ denudation rates, and between $^{10}Be_i$ sediment fluxes, $^{10}Be_m/^{9}Be_{reac}$ denudation rates, and historical sediment yields.

Valette-Silver et al. (1986) showed that topsoil erosion associated with European-American deforestation (Brush, 2009) led to deposition of post-colonial sediment in the northern arm of Chesapeake Bay, fed by the Susquehanna River. $^{10}Be_m$ concentrations associated with these post-colonial sediments (7–11 x 10^8 atoms g^{-1}) were well above pre-colonial $^{10}Be_m$ concentrations (2 x 10^8 atoms g^{-1}). After colonial-era erosion removed many centimeters of near-surface topsoil (Costa, 1975), likely containing the highest $^{10}Be_m$ concentrations (Graly et al., 2010), concentrations of $^{10}Be_m$ on sediment delivered to Chesapeake Bay dropped to ~5 x10^8 atoms g^{-1}. Few $^{10}Be_m$ measurements in our Potomac River samples have concentrations <2 x 10^8 atoms g^{-1} or >5 x 10^8 atoms g^{-1}.

Considering that similar land-use practices were used in both the Susquehanna and Potomac watersheds during the colonial era, it is likely that that ^{10}Be-enriched topsoil in the basins delivering sediment to our sample sites was eroded just after settlement. $^{10}Be_m$ concentration in river sediment now reflects $^{10}Be_m$-depleted parts of soil profiles, the highest concentration material having been swept downstream and into the Bay during and after colonial and post-colonial land clearance.

A sediment core collected at the mouth of Chesapeake Bay, downstream from the tidal Potomac River, however, shows $^{10}Be_m$ measurements of <5 x 10^8 atoms g^{-1} (Helz and Valette-Silver, 1992) – i.e. no colonial-era $^{10}Be_m$ spike is observed. Thus, if $^{10}Be_m$ in topsoil was eroded from sampled basins, much of the $^{10}Be_m$ has not yet reached the mouth of Chesapeake Bay, >200 km downstream from the mouth of the non-tidal Potomac River. We suggest that the lost $^{10}Be_m$ is likely stored within river sub-basins, both behind milldams in the field area (Merritts et al., 2011; Walter and Merritts, 2008) and on colluvial footslopes (Reusser et al., 2015), an interpretation that is strongly supported by erosion indices derived for much of our field area that indicate sediment storage (Fig. 6). Eroded topsoil sediment and the $^{10}Be_m$ adhered to it may reside near the mouth of the Potomac River, much like the $^{10}Be_m$ spike Valette-Silver et al. (1986) identified for Chesapeake Bay was found proximal to the mouth of the Susquehanna River; however, this hypothesis remains untested.

The lack of clear and expected anticorrelation between the $^{10}Be_m/^9Be_{reac}$ ratios and $^{10}Be_i$ erosion rate data sets in the Potomac River basin (Fig. 5), the dissimilarity between $^{10}Be_m$ and $^{10}Be_i$ erosion rates, and between $^{10}Be_m/^9Be_{reac}$ denudation rates and $^{10}Be_i$ erosion rates may reflect noise inherent to the $^{10}Be_m$ system, the limited dynamic range of erosion rates (meters to tens of meters per million years) in the Potomac basin, and the lack of grainsize-specific isotopic and sediment transport flux data. A similar comparative analysis in the much larger Amazon Basin, where erosion rates vary over three orders of magnitude, showed what appeared to be a more pronounced inverse relationship between $^{10}Be_m/^9Be_{reac}$ ratios and $^{10}Be_i$ physical sediment fluxes as well as other metrics of erosion (Fig. 6 in von Blanckenburg et al., 2012). However, the scatter of $^{10}Be_m/^9Be_{reac}$ sediment generation rates in the Potomac River basin (Fig. 3d) is similar to scatter of $^{10}Be_m/^9Be_{reac}$ sediment generation rates within the same range (10–100 Mg km^{-2} yr^{-1}) for various river basins in North America (Fig. 3f). Together, these findings suggest that the scatter within the $^{10}Be_m/^9Be_{reac}$ data set is inherent to the interpretation of $^{10}Be_m/^9Be_{reac}$ ratios as denudation rates. This is a key finding shared between our work and previous studies and suggests that the meaningful application of $^{10}Be_m/^9Be_{reac}$ denudation rates will be limited to field areas where denudation varies by orders of magnitude. In that case, the relative magnitude of landscape change between one part of a landscape and another can be detected, even if $^{10}Be_m/^9Be_{reac}$ rates from specific catchments do not consistently replicate $^{10}Be_i$ rates.

The overall agreement between mean $^{10}Be_i$ erosion rates and $^{10}Be_m/^9Be_{reac}$ denudation rates, when considering the Potomac River basin sample set as a whole, suggests that $^{10}Be_m$ when normalized to $^9Be_{reac}$ could be useful at a broad scale for understanding the pattern and tempo of landscape change in quartz-poor regions where $^{10}Be_i$ is not suitable (e.g. Dannhaus et al., 2018). However, until $^{10}Be_m/^9Be_{reac}$ denudation rates can be shown to routinely replicate $^{10}Be_i$-determined rates in sub-basins where both techniques should be expected to track the same landscape dynamics (i.e. landscapes with soil depths equal to or shallower than the spallogenic cosmogenic nuclide production depth), $^{10}Be_m/^9Be_{reac}$ denudation rates at the sub-basin scale appear to have limited utility. Based on the Potomac River data set, it appears that applying the $^{10}Be_m/^9Be_{reac}$ denudation rate technique to landscapes with intensive human land-use histories (most of the currently developed world where land clearance and intensive agriculture have been practiced) is problematic.

Long-Term, Background Erosion Rates and Landscape Change

Using the data presented here, sediment dynamics in the Potomac River watershed and sediment delivery to Chesapeake Bay, can now be assessed in the context of long-term landscape change rates within the river catchment. Measurements of $^{10}Be_i$ show that the Potomac River basin erodes slowly over millennial timescales (11.0 ± 5.2 m m.y.$^{-1}$, assuming a rock density of 2,700 kg m^{-3}), closely replicating the range of basin-averaged erosion rates from the nearby Shenandoah National Park (12.2 ± 4.6 m m.y.$^{-1}$; Duxbury et al., 2015). However, the Potomac River basin is, on average, eroding at nearly half the pace as unglaciated parts of the Susquehanna River basin to the north (19.7 m m.y.$^{-1}$; Reuter, 2005), which is interesting because the Susquehanna basin is underlain by the same physiographic provinces and bedrock lithologies, and has experienced a similar history of human land use. The two-fold difference in average long-term erosion rates between the Potomac and Susquehanna River watersheds may reflect either a base-level change affecting only the Susquehanna (i.e. Miller et al., 2013) or the closer proximity of many of the Susquehanna sub-basins to the former Laurentide glacial margin, where they experienced more intense periglacial weathering (Clark and Ciolkosz, 1988; Denn et al., 2018; Marshall et al., 2015; Whittecar and Ryter, 1992). We consider the latter of these explanations to be dominant as we interpret the positive relationship between erosion rates and latitude in the Potomac basin (Fig. 2) to reflect increased periglacial activity closer to the former glacial margin.

$^{10}Be_i$-determined erosion rates are similar to but somewhat lower than rock exhumation rates measured using apatite and zircon fission-track and (U-Th)/He dating techniques (Naeser et al., 2016; Reed et al., 2005; ~15–25 m m.y.$^{-1}$) over >10^6 yr timescales in the Potomac region of the central Appalachian Mountains. From this comparison of erosion rates, we infer that the pace of landscape denudation in the Potomac River basin is similar when integrated over 10^4–10^6 yr timescales. The observed consistency of erosion and denudation rates over different timescales is similar to that found by Matmon et al. (2003) in the Great Smoky Mountains further to the south, suggesting long-term stable rates of landscape change over time throughout the non-glaciated Appalachian Mountains.

A comparison of $^{10}Be_i$ basin-averaged and outcrop-specific erosion rates suggests that relief is generally not being generated throughout most of the Potomac River basin, supporting our interpretation of long-term stable rates of landscape change. Along with data from this study, $^{10}Be_i$ erosion rates from basins draining the western flank of the Blue Ridge in Shenandoah National Park (Duxbury et al., 2015) and from bedrock outcrops along ridgelines throughout the Potomac River watershed (Duxbury et al., 2015; Hancock et al., 2015; Portenga et al., 2013) show that average erosion rates of basins and outcrops in the Valley and Ridge and the Blue Ridge Provinces are similar within 1σ uncertainties (Fig. 7). Outcrop erosion rates from the Appalachian Plateau are not available for the Potomac River watershed; however, $^{10}Be_i$ erosion rates of outcrops west of the continental divide in Dolly Sods, West Virginia (Hancock and Kirwan, 2007), are similar to outcrop erosion rates to the north in the Appalachian Plateau Province within the Susquehanna River basin (Portenga et al., 2013; Reuter, 2005), and so we consider these reasonable estimates of rock erosion in the Appalachian Plateau of the Potomac River watershed. When bedrock erosion rates from Dolly Sods and the Susquehanna Appalachian Plateau are assumed representative of outcrop erosion in the Potomac Appalachian Plateau, we identify and interpret the largest difference between outcrop and basin-averaged $^{10}Be_i$ erosion rates in the Potomac River watershed to reflect relief generation in the Appalachian Plateau (Fig. 7). Our observations of erosion rate difference and inferred relief generation in the Potomac Appalachian Plateau are consistent with base-level fall following stream capture west of the Blue Ridge and knickpoint retreat into headwater basins along the continental divide, as has been demonstrated for the central Appalachian Mountains (Miller et al., 2013; Naeser et al., 2016; Prince et al., 2010, 2011).

Erosion Indices

EIs of distal headwater basins indicate that more $^{10}Be_m$ is being exported from the Appalachian Plateau Province than is being retained on the landscape. This observation supports findings presented in this study that relief is being produced in the Appalachian Plateau Province and is consistent with Miller et al.'s (2013) findings that stream incision in the central Appalachian Mountains is greatest in headwater catchments along the continental divide. Conversely, EIs of the large basins (samples POT01 and POT06/USGS 01638500) indicate that $^{10}Be_m$ is being retained within the Potomac River basin. Since there are few large dams on the main branch of the Potomac River to trap sediment (Gerhart, 1991), we suggest this $^{10}Be_m$ is likely stored in the floodplain or in colluvium below hillslopes; alternatively, $^{10}Be_m$-bearing sediment eroded from headwater streams may have become trapped behind numerous small milldams as legacy sediment (Merritts et al., 2011; Walter and Merritts, 2008) and is now being released, or will be released in the future, to the larger Potomac River basin as these milldams deteriorate. Basins with high EIs and high long-term erosion rates (e.g., POT11, USGS gauging station 01610200) are those where increased sediment delivery reflects downcutting by headwaters of the Potomac River watershed. High EIs in basins corresponding to low long-term sediment yields (POT13) reflect agricultural land use where topsoil, having long near-surface residence time (i.e., low sediment yields derived from high $^{10}Be_i$ concentrations), is eroded and carries with it large amounts of $^{10}Be_m$. $^{10}Be_m$ retention (EI < 1) seems also to occur in urban centers around Washington, DC (POT02–POT05) – a perplexing finding considering that sediment yields from local urban catchments are some of the highest in the Chesapeake Bay watershed (Gellis et al., 2017). The possibility of significant amounts of foreign sediment being brought into, or native sediment being exported from urban sampled basins cannot be excluded, though it is difficult to quantify such activities.

The equivalence between the EIs calculated for the main branch of the Potomac River from this study and from Brown et al. (1988; EI = 0.55 for POT06 and EI = 0.58 for USGS gauging station 01638500, respectively) is notable, considering that we only used the 250–850 μm grain size whereas Brown et al. (1988) used unsieved samples. Such a similarity between EIs supports our earlier assertion that our $^{10}Be_m/^{9}Be_{reac}$ data set is not significantly affected by grain-size bias and shows replication in EIs from samples collected decades apart.

Because paleo-sediment loads and $^{10}Be_m$ paleo-flux rates are not known for the 13 samples collected from the Hybla Valley sediment core, past EIs for the whole of the Potomac River cannot be derived. However, we can still infer past landscape dynamics by assessing how measured $^{10}Be_m$ concentrations change through time in the Hybla Valley core (Fig. 8; cf. Helz and Valette-Silver, 1992; Valette-Silver et al., 1986; van Geen et al., 1999). If we assume $^{10}Be_m$ flux rates during the late Pleistocene have fluctuated around an average value, $^{10}Be_m$ concentrations on sediment delivered to the lower Potomac River would only increase significantly as a result of increased topsoil erosion rates, supplying more sediment to Chesapeake Bay (i.e. Valette-Silver et al., 1986). Under this assumption, the long-term trend of $^{10}Be_m$ concentrations from the Hybla Valley suggest that soil erosion was more intense and sediment delivery to the Bay increased during cold glacial periods over the last ~100 k.y. as indicated by decreases in abundances of oak (*Quercus* spp.), which thrives in relatively warmer climates (Litwin et al., 2013). Relative to modern $^{10}Be_m$ concentrations, low $^{10}Be_m$ concentrations are observed at ca. 80–70 ka, when oak abundances were at their greatest, indicating the warmest climate. Similarly, low $^{10}Be_m$ concentrations are observed at the top of the Hybla Core, perhaps reflecting the current interglacial warming trend. While the inferred increases in $^{10}Be_m$ and sediment export during colder climates was likely facilitated by increased periglacial activity, changes in $^{10}Be_m$ concentrations over the last ~100 k.y. may reflect changes in storm frequency and/or magnitude over glacial/interglacial cycles. Modern $^{10}Be_m$ concentrations from the most downstream Potomac River sample (POT01) are similar in magnitude to van Geen et al.'s (1999) observations at the mouth of Chesapeake Bay, and may reflect intensive colonial-era land use, depletion of topsoils, and exhaustion of upstream $^{10}Be_m$ soil inventories, as discussed above.

Implications of the Isotopic Data for Contextualizing Sediment Delivery to Chesapeake Bay

Efforts to restore the ecology of Chesapeake Bay to a pre-disturbance condition highlight the importance of reducing sediment delivery to the Bay (Hassett et al., 2005; Langland and Cronin, 2003), but to what level? Total maximum daily loads (TMDLs) are regulatory benchmarks for sediment delivery, derived from a combination of measured sediment yields in less disturbed basins and various land-use models (U.S. EPA, 2010). Currently, the target suspended sediment TMDL for the whole of the Potomac River basin is 24.3 Mg km^{-2} yr^{-1} (U.S. EPA, 2010), which is within the uncertainties of the long-term $^{10}Be_i$-derived sediment flux (29.6 ± 14.1 Mg km^{-2} yr^{-1}, 1σ). Because the $^{10}Be_i$-inferred sediment flux for the Potomac River integrates over tens of thousands of years, it is more representative of background sediment delivery from the Potomac River to Chesapeake Bay than shorter-term sediment yields (e.g., Gellis et al., 2004) or sediment deposition rates calculated from sediment cores extracted from the Bay (e.g., Brush, 1984; Cooper and Brush, 1991, 1993; Cronin et al., 1999, 2000; Valette-Silver et al., 1986).

CONCLUSIONS

The $^{10}Be_i$-derived erosion and thus sediment flux rates in this study provide limits on the long-term delivery rate of mass from the Potomac River to Chesapeake Bay. We find that average $^{10}Be_i$ erosion rates and $^{10}Be_m/^9Be_{reac}$-derived denudation rates are similar. However, $^{10}Be_m/^9Be_{reac}$ denudation rates do not replicate $^{10}Be_i$-based erosion rates well when comparing sub-basins; similarly, we find that on average $^{10}Be_m$ erosion rates are greater than $^{10}Be_m/^9Be_{reac}$ denudation rates, which is not possible and thus likely reflects grainsize bias in non-normalized $^{10}Be_m$ concentrations. Although the $^{10}Be_m$ erosion rate and $^{10}Be_m/^9Be_{reac}$ denudation rate technique may be useful for understanding overall rates of landscape change in quartz-poor regions, the techniques does not replicate ^{10}Be$_{i}$-based data well in the Potomac River basin. It appears that land use impacts of the past centuries removed sediment with the highest ^{10}Be$_{m}$ concentrations biasing the calculations. This is likely to pose a complication with ^{10}Be$_{m}$ data worldwide.

New ^{10}Be$_{i}$ erosion rates for the Potomac River in this study are consistent with those presented in other ^{10}Be$_{i}$ studies throughout the central Appalachian Mountains. Differences between basin-averaged and outcrop erosion are limited to headwaters in the Appalachian Plateau region, where erosion indices indicate net sediment export and where knickpoints are propagating into distal headwater basins. Quaternary sediment delivery from the Potomac River basin, represented by ^{10}Be$_{m}$ concentrations in the Hybla Valley core, appears to reflect regional climate change such that more erosion of ^{10}Be$_{m}$-rich topsoils occurs during colder climatic periods, at least over the last 150 k.y. Over modern timescales, we find that sediment yields still greatly exceed background rates of sediment flux from the Potomac River to Chesapeake Bay, and until these rates are reduced, the ecological health of the Bay will not recover to a pre-disturbance condition. TMDLs regulating sediment delivery from the Potomac River to Chesapeake Bay are set to an appropriate level if the overall goal is to reduce sediment delivery to background rates.

ACKNOWLEDGMENTS

The ^{10}Be$_{m}$ data and ^{10}Be$_{i}$ presented here are from C.D. Trodick's M.S. thesis, University of Vermont (UVM), 2011. The ^{9}Be$_{min}$ extraction techniques, detailed in the supplementary material (see text footnote 1), are from S.E. Greene's M.S. thesis (UVM), 2016. We thank J. Landis at Dartmouth University and N. Perdrial at UVM for sample processing advice ; the staff of the Center for Accelerator Mass Spectrometry at Lawrence Livermore National Laboratory for support during accelerator mass spectrometry analyses; F. von Blanckenburg, J. Bouchez, and H. Wittmann for discussions, guidance on appropriate application of the ^{10}Be$_{m}$/^{9}Be$_{reac}$ techniques, and verification of the ^{10}Be$_{m}$/^{9}Be$_{reac}$ data presented in this study; and two anonymous reviewers for comments. Research supported by U.S. Geological Survey grant 08ERSA0582 and National Science Foundation grant EAR-310208.

REFERENCES CITED

Arkle, J.C., Owen, L.A., Weber, J., Caffee, M.W., and Hammer, S., 2017, Transient Quaternary erosion and tectonic inversion of the Northern Range, Trinidad: Geomorphology, v. 295, p. 337–353, doi:10.1016/j.geomorph.2017.07.013.

Åström, M.E., Yu, C., Peltola, P., Reynolds, J.K., Österholm, P., Nystrand, M.I., Augustsson, A., Virtasalo, J.J., Nordmyr, L., and Ojala, A.E.K., 2018, Sources, transport and sinks of beryllium in a coastal landscape affected by acidic soils: Geochimica et Cosmochimica Acta, doi:10.1016/j.gca.2018.04.025.

Bacon, A.R., Richter, D.D., Bierman, P.R., and Rood, D.H., 2012, Coupling meteoric ^{10}Be with pedogenic losses of ^{9}Be to improve soil residence time estimates on an ancient North American interfluve: Geology, v. 40, no. 9, p. 847–850, doi:10.1130/G33449.1.

Balco, G., Stone, J.O., Lifton, N.A., and Dunai, T.J., 2008, A complete and easily accessible means of calculating surface exposure ages or erosion rates from ^{10}Be and ^{26}Al measurements: Quaternary Geochronology, v. 3, no. 3, p. 174–195, doi:10.1016/j.quageo.2007.12.001.

Barg, E., Lal, D., Pavich, M.J., Caffee, M.W., and Southon, J.R., 1997, Beryllium geochemistry in soils: Evaluation of ^{10}Be/^{9}Be ratios in authigenic minerals as a basis for age models: Chemical Geology, v. 140, no. 3–4, p. 237–258, doi:10.1016/S0009-2541(97)00051-X.

Bierman, P., 2015, The incision history of the Great Falls of the Potomac River—The Kirk Bryan 2015 field trip: Geological Society of America Field Guide 40, p. 1–10, doi:10.1130/2015.0040(01).

Bierman, P., and Steig, E.J., 1996, Estimating rates of denudation using cosmogenic isotope abundances in sediment: Earth Surface Processes and Landforms, v. 21, p. 125–139, doi:10.1002/(SICI)1096-9837(199602)21:2<125::AID-ESP511>3.0.CO;2-8.

Brown, E.T., Edmond, J.M., Raisbeck, G.M., Bourlès, D.L., and Yiou, F., 1992, Beryllium isotope geochemistry in tropical river basins: Geochimica et Cosmochimica Acta, v. 56, no. 4, p. 1607–1624, doi:10.1016/0016-7037(92)90228-B.

Brown, E.T., Stallard, R.F., Larsen, M.C., Raisbeck, G.M., and Yiou, F., 1995, Denudation rates determined from the accumulation of *in situ*–produced ^{10}Be in the Luquillo Experimental Forest, Puerto Rico: Earth and Planetary Science Letters, v. 129, p. 193–202, doi:10.1016/0012-821X(94)00249-X.

Brown, E.T., Stallard, R.F., Larsen, M.C., Bourlès, D.L., Raisbeck, G.M., and Yiou, F., 1998, Determination of predevelopment denudation rates of an agricultural watershed (Cayaguás River, Puerto Rico) using in-situ-produced ^{10}Be in river-borne quartz: Earth and Planetary Science Letters, v. 160, p. 723–728, doi:10.1016/S0012-821X(98)00123-X.

Brown, L., Sacks, I.S., and Tera, F., 1981, Beryllium-10 in continental sediments: Earth and Planetary Science Letters, v. 55, p. 370–376, doi:10.1016/0012-821X(81)90165-5.

Brown, L., Pavich, M.J., Hickman, R.E., Klein, J., and Middleton, R., 1988, Erosion of the eastern United States observed with ^{10}Be: Earth Surface Processes and Landforms, v. 13, no. 5, p. 441–457, doi:10.1002/esp.3290130509.

Brush, G.S., 1984, Patterns of recent sediment accumulation in Chesapeake Bay (Virginia-Maryland, U.S.A.) tributaries: Chemical Geology, v. 44, p. 227–242, doi:10.1016/0009-2541(84)90074-3.

Brush, G.S., 2009, Historical land use, nitrogen, and coastal eutrophication: A paleoecological perspective: Estuaries and Coasts, v. 32, p. 18–28, doi:10.1007/s12237-008-9106-z.

Chmeleff, J., von Blanckenburg, F., Kossert, K., and Jakob, D., 2010, Determination of the ^{10}Be half-life by multicollector ICP-MS and liquid scintillation counting: Nuclear Instruments and Methods in Physics Research B: Beam Interactions with Materials and Atoms, v. 268, p. 192–199.

Clark, G.M., and Ciolkosz, E.J., 1988, Periglacial geomorphology of the Appalachian highlands and interior highlands south of the glacial border—A review: Geomorphology, v. 1, p. 191–220, doi:10.1016/0169-555X(88)90014-1.

Colman, S.M., and Bratton, J.F., 2003, Anthropogenically induced changes in sediment and biogenic silica fluxes in Chesapeake Bay: Geology, v. 31, no. 1, p. 71–74, doi:10.1130/0091-7613(2003)031<0071:AICISA>2.0.CO;2.

Cooper, S.R., and Brush, G.S., 1991, Long-term history of Chesapeake Bay anoxia: Science, v. 254, p. 992–996, doi:10.1126/science.254.5034.992.

Cooper, S.R., and Brush, G.S., 1993, A 2,500-year history of anoxia and eutrophication in Chesapeake Bay: Estuaries, v. 16, no. 3B, p. 617–626, doi:10.2307/1352799.

Corbett, L.B., Bierman, P.R., and Rood, D.H., 2016, An approach for optimizing *in situ* cosmogenic ^{10}Be sample preparation: Quaternary Geochronology, v. 33, p. 24–34, doi:10.1016/j.quageo.2016.02.001.

Costa, J.E., 1975, Effects of agriculture on erosion and sedimentation in the Piedmont Province, Maryland: Geological Society of America Bulletin, v. 86, p. 1281–1286, doi:10.1130/0016-

7606(1975)86<1281:EOAOEA>2.0.CO;2.

Cronin, T., Colman, S., Willard, D., Kerhin, R., Holmes, C., Karlsen, A., Ishman, S., and Bratton, J., 1999, Interdisciplinary environmental project probes Chesapeake Bay down to the core: Eos (Washington, D.C.), v. 80, no. 221, p. 237–240.

Cronin, T., Willard, D., Karlsen, A., Ishman, S., Verardo, S., McGeehin, J., Kerhin, R., Holmes, C., Colman, S., and Zimmerman, A., 2000, Climatic variability in the eastern United States over the past millennium from Chesapeake Bay sediments: Geology, v. 28, no. 1, p. 3–6, doi:10.1130/0091-7613(2000)28<3:CVITEU>2.0.CO;2.

Dannhaus, N., Wittmann, H., Krám, P., Christl, M., and von Blanckenburg, F., 2018, Catchment-wide weathering and erosion rates of mafic, ultramafic, and granitic rock from cosmogenic meteoric ^{10}Be/^{9}Be ratios: Geochimica et Cosmochimica Acta, v. 222, p. 618–641, doi: 10.1016/j.gca.2017.11.005.

Dauer, D.M., Ranasinghe, J.A., and Weisberg, S.B., 2000, Relationships between benthic community condition, water quality, sediment quality, nutrient loads, and land use patterns in Chesapeake Bay: Estuaries, v. 23, no. 1, p. 80–96, doi:10.2307/1353227.

DeJong, B.D., Bierman, P.R., Newell, W.L., Rittenour, T.M., Mahan, S.A., Balco, G., and Rood, D.H., 2015, Pleistocene relative sea levels in the Chesapeake Bay region and their implications for the next century: GSA Today, v. 25, no. 8, p. 4–10, doi:10.1130/GSATG223A.1.

Denn, A.R., Bierman, P.R., Zimmerman, S.R.H., Caffee, M.C., Corbett, L.B., and Kirby, E., 2018, Cosmogenic nuclides indicate that boulder fields are dynamic, ancient, multigenerational features: GSA Today, v. 28, no. 3–4, p.4–10, doi: 10.1130/GSATG340A.1.

Dixon, J.L. and Chadwick, O., 2017, Insights into meteoric ^{10}Be dynamics and climate stability along the Hawaiian Kohala climosequence: AGU Fall Meeting Abstracts.

Duxbury, J., Bierman, P.R., Portenga, E.W., Pavich, M.J., Southworth, S., and Freeman, S.P.H.T., 2015, Erosion rates in and around Shenandoah National Park, Virginia, determined using analysis of cosmogenic ^{10}Be: American Journal of Science, v. 315, no. 1, p. 46–76, doi:10.2475/01.2015.02.

Frank, M., Backman, J., Jakobsson, M., Moran, K., O'Regan, M., King, J., Haley, B.A., Kubik, P.W., and Garbe-Schönberg, D., 2008, Beryllium isotopes in central Arctic Ocean sediment over the 12.3 million years: Stratigraphic and paleoclimatic implications: Paleoceanography, v. 23, no. 1, p. PA1S02, doi:10.1029/2007PA001478.

Gellis, A.C., Banks, W.S.L., Langland, M.J., and Martucci, S.K., 2004, Summary of Suspended-Sediment Data for Streams Draining the Chesapeake Bay Watershed, Water Years 1952–2002: U.S. Department of the Interior, U.S. Geological Survey, 66 p.

Gellis, A.C., Myers, M.K., Noe, G.B., Hupp, C.R., Schenk, E.R., and Myers, L., 2017, Storms, channel changes, and a sediment budget for an urban-suburban stream, Difficult Run, Virginia, USA: Geomorphology, v. 278, p. 128–148, doi:10.1016/j.geomorph.2016.10.031.

Gerhart, J. M., 1991, National Water-Quality Assessment–Potomac River Basin: U.S. Geological Survey, 3 p.

Graly, J.A., Bierman, P.R., Reusser, L.J., and Pavich, M.J., 2010, Meteoric ^{10}Be in soil profiles—A global meta-analysis: Geochimica et Cosmochimica Acta, v. 74, no. 23, p. 6814–6829, doi:10.1016/j.gca.2010.08.036.

Graly, J.A., Reusser, L.J., and Bierman, P.R., 2011, Short and long-term delivery rates of meteoric ^{10}Be to terrestrial soils: Earth and Planetary Science Letters, v. 302, no. 3–4,

p. 329–336, doi:10.1016/j.epsl.2010.12.020.

Granger, D.E., Kirchner, J.W., and Finkel, R., 1996, Spatially averaged long-term erosion rates measured from *in situ*–produced cosmogenic nuclides in alluvial sediment: The Journal of Geology, v. 104, no. 3, p. 249–257, doi:10.1086/629823.

Greene, E.S., 2016, Comparing Meteoric ^{10}Be, *In situ* ^{10}Be, and Native ^{9}Be Across a Diverse Set of Watersheds [M.S. thesis]: Burlington, Vermont, University of Vermont, 110 p.

Hancock, G., and Kirwan, M., 2007, Summit erosion rates deduced from ^{10}Be: Implications for relief production in the central Appalachians: Geology, v. 35, no. 1, p. 89–92, doi:10.1130/G23147A.1.

Hancock, G.S., Whitten, J., Shintani, C., and Southworth, S., 2015, ^{10}Be-derived bare-bedrock erosion rates on ridgelines imply landscape transience in the Blue Ridge, Shenandoah National Park, Virginia: Geological Society of America Abstracts with Programs, v. 47, no. 7, p. 43.

Harel, M.-A., Mudd, S.M., and Attal, M., 2016, Global analysis of the stream power law parameters based on worldwide ^{10}Be denudation rates: Geomorphology, v. 268, p. 184–196, doi:10.1016/j.geomorph.2016.05.035.

Hassett, B., Palmer, M., Bernhardt, E., Smith, S., Carr, J., and Hart, D., 2005, Restoring watersheds project by project: Trends in Chesapeake Bay tributary restoration: Frontiers in Ecology and the Environment, v. 3, no. 5, p. 259–267, doi:10.1890/1540-9295(2005)003[0259:RWPBPT]2.0.CO;2.

Heikkilä, U., and von Blanckenburg, F, 2015, . Distribution maps for terrestrial Earth surface applications. GFZ Data Services, doi:10.5880/GFZ.3.4.2015.001.

Heimsath, A.M., Chappell, J., Finkel, R.C., Fifield, K., and Alimanovic, A., 2006, Escarpment erosion and landscape evolution in southeastern Australia, *in* Willett, S.D., Hovius, N., Brandon, M.T., and Fisher, D.M., eds., Tectonics, Climate, and Landscape Evolution: Geological Society of America Special Paper 398, p. 173–190, doi:10.1130/2006.2398(10).

Helz, G.R., and Valette-Silver, N., 1992, Beryllium-10 in Chesapeake Bay sediments: An indicator of sediment provenance: Estuarine, Coastal and Shelf Science, v. 34, no. 5, p. 459–469, doi:10.1016/S0272-7714(05)80117-9.

Hijmans, R.J., Cameron, S.E., Parra, J.L., Jones, P.G., and Jarvis, A., 2005, Very high resolution interpolated climate surfaces for global land areas: International Journal of Climatology, v. 25, p. 1965–1978, doi:10.1002/joc.1276.

Hooke, R.L., Martin-Duque, J.F., and Pedraza, J., 2012, Land transformation by humans: A review: GSA Today, v. 22, no. 12, p. 4–10, doi:10.1130/GSAT151A.1.

Ives, J.D., 1978, The maximum extent of the Laurentide ice sheet along the east coast of North America during the last glaciation: Arctic, v. 31, no. 1, p. 24–53, doi:10.14430/arctic2638.

Jonell, T.N., Clift, P.D., Hoang, L.V., Hoang, T., Carter, A., Wittmann, H., Böning, P., Pahnke, K., and Rittenour, T., 2016, Controls on erosion patterns and sediment transport in a monsoonal, tectonically quiescent drainage, Song Gianh, central Vietnam: Basin Research, v. 29, no. S1, 659–683, doi:10.1111/bre.12199.

Judson, S., 1968, Erosion of the land, or what's happening to our continents?: American Scientist, v. 56, no. 4, p 356–374.

Kirby, M.X., 2004, Fishing down the coast: Historical expansion and collapse of oyster fisheries along continental margins: Proceedings of the National Academy of Sciences of the United States of America, v. 101, no. 35, p. 13,096–13,099, doi:10.1073/pnas.0405150101.

Kirchner, J.W., Finkel, R.C., Riebe, C.S., Granger, D.E., Clayton, J.L., King, J.G., and Megahan, W.F., 2001, Mountain erosion over 10 yr, 10 k.y., and 10 m.y. time scales: Geology, v. 29, no. 7, p. 591–594, doi:10.1130/0091-7613(2001)029<0591:MEOYKY>2.0.CO;2.

Korschinek, G., Bergmaier, A., Faestermann, T., Gerstmann, U.C., Knie, K., Rugel, G., Wallner, A., Dillmann, I., Dollinger, G., von Gostomski, C.L., Kossert, K., Maiti, M., Poutivtsev, M., and Remmert, A., 2010, A new value for the half-life of ^{10}Be by heavy-ion elastic recoil detection and liquid scintillation counting: Nuclear Instruments and Methods in Physics Research B: Beam Interactions with Materials and Atoms, v. 268, p. 187–191.

Kusakabe, M., Ku, T.L., Southon, J.R., Liu, S., Vogel, J.S., Nelson, D.E., and Nakaya, S., 1991, Be isotopes in rivers/estuaries and their oceanic budgets: Earth and Planetary Science Letters, v. 102, no. 3–4, p. 265–276, doi:10.1016/0012-821X(91)90022-A.

Lal, D., 1991, Cosmic ray labeling of erosion surfaces: *In situ* nuclide production rates and erosion models: Earth and Planetary Science Letters, v. 104, no. 2–4, p. 424–439, doi:10.1016/0012-821X(91)90220-C.

Lal, D., and Peters, B., 1962, Cosmic ray produced isotopes and their application to problems in geophysics, *in* Wilson, J.G., and Wouthysen, S.A., eds., Progress in Elementary Particle and Cosmic Ray Physics: New York, Wiley, p. 1–74.

Langland, M., and Cronin, T., 2003, A Summary Report of Sediment Processes in the Chesapeake Bay and Watershed: U.S. Geological Survey Water Resources Investigation Report 03–4123, 122 p.

Langland, M.J., and Hainly, R.A., 1997, Changes in bottom-surface elevations in three reservoirs on the lower Susquehanna River, Pennsylvania and Maryland, following the January 1996 flood—Implications for nutrient and sediment loads to Chesapeake Bay, *in* Linari, C.L., Bierman, P.R., Portenga, E.W., and Pavich, M.J., eds., Erosion and Landscape Evolution of the Blue Ridge Escarpment, Southern Appalachian Mountains: U.S. Geological Survey Water Resources Investigation Report 97-4138, 34 p.

Linari, C.L., Bierman, P.R., Portenga, E.W., Pavich, M.J., Finkel, R.C., and Freeman, S.P.H.T., 2016, Rates of erosion and landscape change along the Blue Ridge escarpment, southern Appalachian Mountains, estimated from *in situ* cosmogenic ^{10}Be: Earth Surface Processes and Landforms, doi:10.1002/esp.4051.

Litwin, R.J., Smoot, J.P., Pavich, M.J., Markewich, H.W., Brook, G., and Durika, N.J., 2013, 100,000-year-long terrestrial record of millennial-scale linkage between eastern North American mid-latitude paleovegetation shifts and Greenland ice-core oxygen isotope trends: Quaternary Research, v. 80, no. 2, p. 291–315, doi:10.1016/j.yqres.2013.05.003.

Mandal, S.K., Lupker, M., Burg, J.-P., Valla, P.G., Haghipour, N., and Christl, M., 2015, Spatial variability of ^{10}Be-derived erosion rates across the southern Peninsular Indian escarpment: A key to landscape evolution across passive margins: Earth and Planetary Science Letters, v. 425, p. 154–167, doi:10.1016/j.epsl.2015.05.050.

Marshall, J.A., Roering, J.J., Bartlein, P.J., Gavin, D.G., Granger, D.E., Rempel, A.W., Praskievicz, S.J., and Hales, T.C., 2015, Frost for the trees: Did climate increase erosion in unglaciated landscapes during the late Pleistocene?: Science Advances, v. 1, no. 10, p. e1500715, doi:10.1126/sciadv.1500715.

Matmon, A., Bierman, P.R., Larsen, J., Southworth, S., Pavich, M., Finkel, R., and Caffee, M., 2003, Erosion of an ancient mountain range, the Great Smoky Mountains, North Carolina and Tennessee: American Journal of Science, v. 303, no. 9, p. 817–855, doi:10.2475/ajs.303.9.817.

McLennan, S.M., 1993, Weathering and global denudation: The Journal of Geology, v. 101, no.

2, p. 295–303.

Merritts, D., Walter, R., Rahnis, M., Hartranft, J., Cox, S., Gellis, A., Potter, N., Hilgartner, W., Langland, M., Manion, L., Lippincott, C., Siddiqui, S., Rehman, Z., Scheid, C., Kratz, L., Shilling, A., Jenschke, M., Datin, K., Cranmer, E., Reed, A., Matuszewski, D., Voli, M., Ohlson, E., Neugebauer, A., Ahamed, A., Neal, C., Winter, A., and Becker, S., 2011, Anthropocene streams and base-level controls from historic dams in the unglaciated Mid-Atlantic region, USA: Philosophical Transactions of the Royal Society A: Mathematical, Physical and Engineering Sciences, v. 369, no. 1938, p. 976–1009.

Middleton, R., Brown, L., Dezfouly-Arjomandy, B., and Klein, J., 1993, On ^{10}Be standards and the half-life of ^{10}Be: Nuclear Instruments and Methods in Physics Research B, v. 82, p. 399–403. doi:10.1016/0168-583X(93)95987-G.

Miller, S.R., Sak, P.B., Kirby, E., and Bierman, P.R., 2013, Neogene rejuvenation of central Appalachian topography: Evidence for differential rock uplift from stream profiles and erosion rates: Earth and Planetary Science Letters, v. 369–370, p. 1–12, doi:10.1016/j.epsl.2013.04.007.

Milliman, J.D., and Syvitski, J.P.M., 1992, Geomorphic/tectonic control of sediment discharge to the ocean: The importance of small mountainous rivers: the Journal of Geology, v. 100, no. 5, p. 525–544.

Montgomery, D.R., 2007, Dirt: The Erosion of Civilizations: Berkeley, California, University of California Press, 295 p.

Naeser, C.W., Naeser, N.D., Newell, W.L., Southworth, S., Edwards, L.E., and Weems, R.E., 2016, Erosional and depositional history of the Atlantic passive margin as recorded in detrital zircon fission-track ages and lithic detritus in Atlantic Coastal Plain sediments: American Journal of Science, v. 316, p. 110–168.

Nishiizumi, K., Lal, D., Klein, J., Middleton, R., and Arnold, J.R., 1986, Production of ^{10}Be and ^{26}Al by cosmic rays in terrestrial quartz *in situ* and implications for erosion rates: Nature, v. 319, p. 134–136, doi:10.1038/319134a0.

Nishiizumi, K., Imamura, M., Caffee, M.W., Southon, J.R., Finkel, R.C., and McAninch, J., 2007, Absolute calibration of ^{10}Be AMS standards: Nuclear Instruments and Methods in Physics Research B: Beam Interactions with Materials and Atoms, v. 258, no. 2, p. 403–413.

NOAA, 2010, Online Coastal Geospatial Data Project, http://coastalgeospatial.noaa.gov/data_gis.html (last accessed 21 July 2011; now accessible at https://coas.noaa.gov/digitalcoast/).

Ouimet, W.B., Whipple, K.X., and Granger, D.E., 2009, Beyond threshold hillslopes: Channel adjustment to base-level fall in tectonically active mountain ranges: Geology, v. 37, no. 7, p. 579–582, doi:10.1130/G30013A.1.

Pavich, M.J., 1989, Regolith residence time and the concept of surface age of the Piedmont "peneplain": Geomorphology, v. 2, p. 181–196, doi:10/1016/0169-555X(89)90011-1.

Pavich, M.J., 1990, Characteristics, origin, and residence time of saprolite and soil of the Piedmont upland, Virginia, U.S.A., and model testing using cosmogenic ^{10}Be: Chemical Geology, v. 84, no. 1/4, p. 15–16.

Pavich, M.J., Brown, L., Valette-Silver, J.N., Klein, J., and Middleton, R., 1985, ^{10}Be analysis of a Quaternary weathering profile in the Virginia Piedmont: Geology, v. 13, no. 1, p. 39–41, doi:10.1130/0091-7613(1985)13<39:BAOAQW>2.0.CO;2.

Pazzaglia, F.J., and Gardner, T.W., 1994, Late Cenozoic flexural deformation of the middle U.S. Atlantic passive margin: Journal of Geophysical Research, v. 99, p. 12,143–12,157, doi:10.1029/93JB03130.

Pelletier, J.D., Murray, A.B., Pierce, J.L., Bierman, P.R., Breshears, D.D., Crosby, B.T., Ellis, M., Foufoula-Georgiou, E., Heimsath, A.M., Houser, C., Lancaster, N., Marani, M., Merritts, D.J., Moore, L.J., Pederson, J.L., Poulos, M.J., Rittenour, T.M., Rowland, J.C., Ruggiero, P., Ward, D.J., Wickert, A.D., and Yager, E.M., 2015, Forecasting the response of Earth's surface to future climatic and land use changes: A review of methods and research needs: Earth's Future, v. 3, p. 220–251, doi:10.1002/2014EF000290.

Peltier, W.R., 1996, Global sea level rise and glacial isostatic adjustment: An analysis of data from the east coast of North America: Geophysical Research Letters, v. 23, no. 7, p. 717–720, doi:10.1029/96GL00848.

Poag, C.W., and Sevon, W.D., 1989, A record of Appalachian denudation in postrift Mesozoic and Cenozoic sedimentary deposits of the U.S. Middle Atlantic continental margin: Geomorphology, v. 2, p. 119–157, doi:10.1016/0169-555X(89)90009-3.

Portenga, E.W., and Bierman, P.R., 2011, Understanding Earth's eroding surface with ^{10}Be: GSA Today, v. 21, no. 8, p. 4–10, doi:10.1130/G111A.1.

Portenga, E.W., Bierman, P.R., Rizzo, D.M., and Rood, D.H., 2013, Low rates of bedrock outcrop erosion in the central Appalachian Mountains inferred from *in situ* ^{10}Be: Geological Society of America Bulletin, v. 125, no. 1–2, p. 201–215, doi:10.1130/B30559.1.

Portenga, E.W., Bishop, P., Rood, D.H., and Bierman, P.R., 2017, Combining bulk sediment OSL and meteoric ^{10}Be fingerprinting techniques to identify gully initiation sites and erosion depths: Journal of Geophysical Research Earth Surface, v. 122, no. 2, p. 513–527, doi:10.1022/2016JF004052.

Prince, P.S., Spotila, J.A., and Henika, W.S., 2010, New physical evidence of the role of stream capture in active retreat of the Blue Ridge escarpment, southern Appalachians: Geomorphology, v. 123, no. 3–4, p. 305–319, doi:10.1016/j.geomorph.2010.07.023.

Prince, P.S., Spotila, J.A., and Henika, W.S., 2011, Stream capture as driver of transient landscape evolution in a tectonically quiescent setting: Geology, v. 39, no. 9, p. 823–826, doi:10.1130/G32008.1.

Rahaman, W., Wittmann, H., and von Blanckenburg, F., 2017, Denudation rates and the degree of chemical weathering in the Ganga River basin from ratios of meteoric cosmogenic ^{10}Be to stable ^{9}Be: Earth and Planetary Science Letters, v. 469, p. 156–169, doi: 10.1016/j.epsl.2017.04.001.

Reed, J.S., Spotila, J.A., Eriksson, K.A., and Bodnar, R.J., 2005, Burial and exhumation history of Pennsylvanian strata, central Appalachian basin: An integrated study: Basin Research, v. 17, no. 2, p. 259–268, doi:10.1111/j.1365-2117.2005.00265.x.

Reusser, L.J., and Bierman, P.R., 2010, Using meteoric ^{10}Be to track fluvial sand through the Waipaoa River basin, New Zealand: Geology, v. 38, no. 1, p. 47–50, doi:10.1130/G30395.1.

Reusser, L.J., Bierman, P.R., Pavich, M.J., Zen, E.-A., Larsen, J., and Finkel, R., 2004, Rapid late Pleistocene incision of Atlantic passive-margin river gorges: Science, v. 305, p. 499–502, doi:10.1126/science.1097780.

Reusser, L., Bierman, P., and Rood, D., 2015, Quantifying human impacts on rates of erosion and sediment transport at a landscape scale: Geology, v. 43, no. 2, p. 171–174, doi:10.1130/G36272.1.

Reuter, J.M., 2005, Erosion Rates and Patterns Inferred from Cosmogenic ^{10}Be in the Susquehanna River Basin [M.S. thesis]: Burlington, Vermont, University of Vermont, 172 p.

Riebe, C.S., Kirchner, J.W., and Granger, D.E., 2001, Quantifying quartz enrichment and its consequences for cosmogenic measurements of erosion rates from alluvial sediment and regolith: Geomorphology, v. 40, no. 1–2, p. 15–19, doi:10.1016/S0169-555X(01)00031-9.

Rood, D.H., Hall, S., Guilderson, T.P., Finkel, R.C., and Brown, T.A., 2010, Challenges and opportunities in high-precision Be-10 measurements at CAMS: Nuclear Instruments & Methods in Physics Research B: Beam Interactions with Materials and Atoms, v. 268, no. 7–8, p. 730–732, doi:10.1016/j.nimb.2009.10.016.

Rood, D.H., Brown, T.A., Finkel, R.C., and Guilderson, T.P., 2013, Poisson and non-Poisson uncertainty estimations of ^{10}Be/^{9}Be measurements at LLNL–CAMS: Nuclear Instruments & Methods in Physics Research B: Beam Interactions with Materials and Atoms, v. 294, p. 426–429.

Saenger, C., Cronin, T.M., Willard, D., Halka, J., and Kerhin, R., 2008, Increased terrestrial to ocean sediment and carbon fluxes in the northern Chesapeake Bay associated with twentieth century land alteration: Estuaries and Coasts, v. 31, p. 492–500, doi:10.1007/s12237-008-9048-5.

Schaller, M., von Blanckenburg, F., Hovius, N., and Kubik, P.W., 2001, Large-scale erosion rates from *in situ*–produced cosmogenic nuclides in European river sediments: Earth and Planetary Science Letters, v. 188, no. 3–4, p. 441–458, doi:10.1016/S0012-821X(01)00320-X.

Singleton, A.A, Schmidt, A.H., Bierman, P.R., Rood, D.H., Neilson, T.B., Greene, E.S., Bower, J.A., and Perdrial, N., 2016, Effects of grain size, mineralogy, and acid-extractable grain coatings on the distribution of the fallout radionuclides ^{7}Be, ^{10}Be, ^{137}Cs, and ^{210}Pb in river sediment: Geochimica et Cosmochimica Acta, doi:10.1016/j.gca.2016.10.007.

Stone, J., 1998, A rapid fusion method for separation of beryllium-10 from soils and silicates: Geochimica et Cosmochimica Acta, v. 62, no. 3, p. 555–561, doi:10.1016/S0016-7037(97)00340-2.

Stone, J.O., 2000, Air pressure and cosmogenic isotope production: Journal of Geophysical Research, v. 105, no. B10, p. 23,753–723,759.

Struth, L., Teixell, A., Owen, L.A., and Babault, J., 2017, Plateau reduction by drainage divide migration in the Eastern Cordillera of Colombia defined by morphometry and ^{10}Be terrestrial cosmogenic nuclides: Earth Surface Processes and Landforms, v. 42, p. 1155–1170, doi:10.1002/esp.4079.

U.S. Environmental Protection Agency (EPA), 2010, Chesapeake Bay Total Maximum Daily Load for Nitrogen, Phosphorus and Sediment: U.S. Environmental Protection Agency, 352 p.

Valette-Silver, J.N., Brown, L., Pavich, M., Klein, J., and Middleton, R., 1986, Detection of erosion events using ^{10}Be profiles: Example of the impact of agriculture on soil erosion in the Chesapeake Bay area (U.S.A.): Earth and Planetary Science Letters, v. 80, no. 1–2, p. 82–90, doi:10.1016/0012-821X(86)90021-X.

van Geen, A., Valette-Silver, N.J., Luoma, S.N., Fuller, C.C., Baskaran, M., Tera, F., and Klein, J., 1999, Constraints on the sedimentation history of San Francisco Bay from ^{14}C and ^{10}Be: Marine Chemistry, v. 64, no. 1–2, p. 28–38.

von Blanckenburg, F., Bouchez, J., and Wittmann, H., 2012, Earth surface erosion and weathering from the ^{10}Be (meteoric)/^{9}Be ratio: Earth and Planetary Science Letters, v. 351–352, p. 295–305, doi:10.1016/j.epsl.2012.07.022.

Walter, R.C., and Merritts, D.J., 2008, Natural streams and the legacy of water-powered mills: Science, v. 319, no. 5861, p. 299–304, doi:10.1126/science.1151716.

Wear, D.N., and Greis, J.G., 2002, The Southern Forest Resource Assessment Summary Report: U.S. Department of Agriculture Forest Service, 114 p.

Whittecar, G.R., and Ryter, D.W., 1992, Boulder streams, debris fans, and Pleistocene climate change in the Blue Ridge Mountains of central Virginia: The Journal of Geology, v. 100, no. 4, p. 487–494, doi:10.1086/629600.

Willenbring, J.K., and von Blanckenburg, F., 2010, Meteoric cosmogenic beryllium-10 adsorbed to river sediment and soil: Applications for Earth-surface dynamics: Earth-Science Reviews, v. 98, no. 1–2, p. 105–122, doi:10.1016/j.earscirev.2009.10.008.

Willenbring, J.K., Codilean, A.T., and McElroy, B.J., 2013, Earth is (mostly) flat: Apportionment of the flux of continental sediment over millennial time scales: Geology, v. 41, no. 3, p. 343–346, doi:10.1130/G33918.1.

Wittmann, H., von Blanckenburg, F., Maurice, L., Guyot, J.-L., Filizola, N., and Kubik, P.W., 2011, Sediment production and delivery in the Amazon River Basin quantified by *in situ*–produced cosmogenic nuclides and recent river loads: Geological Society of America Bulletin, v. 123, p. 934–950, doi:10.1130/B30317.1.

Wittmann, H., von Blanckenburg, F., Bouchez, J., Dannhaus, N., Naumann, R., Christl, M., and Gaillardet, J., 2012, The dependence of meteoric ^{10}Be concentrations on particle size in Amazon River bed sediment and the extraction of reactive $^{10}Be/^{9}Be$ ratios: Chemical Geology, v. 318–319, p. 126–138, doi:10.1016/j.chemgeo.2012.04.031.

Wittmann, H., von Blanckenburg, F., Dannhaus, N., Bouchez, J., Gaillardet, J., Guyot, J.L., Maurice, L., Roig, H., Filizola, N., and Christl, M., 2015, A test of the cosmogenic ^{10}Be(meteoric)/^{9}Be proxy for simultaneously determining basin-wide erosion rates, denudation rates, and the degree of weathering in the Amazon Basin: Journal of Geophysical Research–Earth Surface, v. 120, p. 2498–2528.

Wolman, M.G., 1967, A cycle of sedimentation and erosion in urban river channels: Geografiska Annaler A: Physical Geography, v. 49, no. 2/4, p. 385–395, doi:10.2307/520904.

You, C.-F., Lee, T., Brown, L., Shen, J.J., and Ju-Chin, C., 1988, ^{10}Be study of rapid erosion in Taiwan: Geochimica et Cosmochimica Acta, v. 52, no. 11, p. 2687–2691, doi:10.1016/0016-7037(88)90037-3.

Figure 1. The location of the Potomac River basin (gray), situated within the Chesapeake Bay drainage basin (bold black line) on the east coast of the United States. Extent of the Last Glacial Maximum (LGM) Laurentide ice sheet is indicated by the stippled gray line. Base map is a world shaded relief map, produced and provided open-access by ESRI. State abbreviations: NY—New York, PA—Pennsylvania, WV—West Virginia, VA—Virginia, DC—District of Columbia, MD—Maryland, DE—Delaware, NJ—New Jersey.

Figure 2. Geographical distribution of $^{10}Be_i$ erosion rates within the Potomac River basin and its contributing tributaries. Open circles are sample sites with $^{10}Be_m$ data, but not $^{10}Be_i$, $^{9}Be_{reac}$, or $^{9}Be_{min}$ data; circles with bull's-eye are sites where $^{10}Be_i$, $^{10}Be_m$, $^{9}Be_{reac}$, and $^{9}Be_{min}$ were measured. Numbers next to sample sites designate the sample ID following the format POTxx. White star is the location of the Hybla Valley sediment core. Black squares are cities: B—Baltimore, Maryland (MD); C—Cumberland, MD; H—Harrisonburg, Virginia (VA); HF—Harpers Ferry, West Virginia (WV); W—Washington, DC. State abbreviations: PA—Pennsylvania, WV—West Virginia, VA—Virginia, MD—Maryland. Dashed lines represent the boundaries between physiographic provinces (water.usgs.gov/GIS/metadata/usgswrd/XML/physio.xml), and the dotted lines are state boundaries. Inset figure shows distribution of sediment generation rates derived from $^{10}Be_i$

DOI:10.1130/B31xxx.1

(black circles), including two statistical outliers (x), which were investigated for the possible introduction of deep-seated sediment introduced to the sample by landscape disturbance; only POT20 (gray outlier) showed signs of heavy landscape disturbance, and thus it is not included in any analyses. Box plot box is bounded by the 25th and 75th quartiles, and the vertical line in the box is the median; box plot whiskers encompass all data between the 25th quartile minus 1.5× the interquartile range and the quartiles plus 1.5× the interquartile range. Base map is a world shaded relief map, produced and provided open-access by ESRI.

Figure 3. (A) Plot of historical sediment yield measured at U.S. Geological Survey gauging stations (Gellis et al., 2004) compared to $^{10}Be_i$-derived sediment fluxes from river sediment collected at the same gauging stations. Contemporary sediment yields are up to 10× greater than $^{10}Be_i$ sediment fluxes. (B) Comparison of $^{10}Be_m$ versus $^{10}Be_i$ erosion rates shows that $^{10}Be_m$ erosion rates do not replicate well the better-understood $^{10}Be_i$ erosion rates and that $^{10}Be_m$ erosion rates are nearly all unsystematically greater than $^{10}Be_i$ erosion rates, except in the Coastal Plain. (C) Concentrations of $^{10}Be_m$ and $^{10}Be_i$ are positively and significantly correlated in the Appalachian Plateau, the Valley and Ridge, and in the Coastal Plain physiographic provinces, but not through the overall data set ($R^2 = 0.044$, $p = 0.104$). (D) Plot of $^{10}Be_m/^{9}Be_{reac}$ denudation rates versus 10Bei-derived sediment fluxes for the Potomac River. The two data sets are weakly correlated (curved dashed black line in log-log space, but denudation rates from individual basins do not replicate $^{10}Be_i$-based sediment fluxes well. (E) Sediment fluxes derived from $^{10}Be_m$-only (eq. 1) versus $^{10}Be_m/^{9}Be_{reac}$ denudation rates (eq. 2). Denudation rates and sediment fluxes are unable to replicate each other, basin-by-basin, even though in a landscape where soils are thin and both measures are based primarily on the same $^{10}Be_m$ measurements. (F) Log-log plot adapted from von Blanckenburg et al. (2012) and updated comparing new mean $^{10}Be_i$- and $^{10}Be_m/^{9}Be_{reac}$-derived sediment generation rates of the Potomac River (white square and black 1σ standard deviation uncertainties; $^{10}Be_i$ sediment generation rate = 29.6 ± 14.1 Mg km^{-2} yr^{-1}; $^{10}Be_m/^{9}Be_{reac}$ sediment generation rate = 40.0 ± 21.7 Mg km^{-2} yr^{-1}) with data derived from sediment yields or $^{10}Be_i$ from other rivers throughout the Arctic (filled gray circles; Frank et al., 2008), the Himalaya region (hollow gray circles; Rahaman et al., 2018), the northern United States (filled black circles; Kusakabe et al., 1991), and South America (hollow black circles; Brown et al., 1992; Wittmann et al., 2011, 2012, 2015). The $^{10}Be_m/^{9}Be_{reac}$ uncertainties are 50% errors of the mean, or as reported in individual studies and $^{10}Be_i$ uncertainties are published uncertainties of sediment generation rates. To plot data from Rahaman et al. (2017) and Wittmann et al. (2015), denudation rates published in units of mm yr^{-1} were multiplied by the published rock density (2,600 kg m^{-3}). The uncertainties of $^{10}Be_m/^{9}Be_{reac}$ sediment generation rates for all basins we sampled in the Potomac River basin represent a large amount of data scatter, similar to estimated 50% uncertainties on means of other North American rivers. For figure panels A-F, error bars as described above are shown; if error bars are not seen, they are smaller than the panel symbology.

Figure 4. Analyses of variance of $^{10}Be_i$ erosion rate data grouped and shaded by (A) land use and (B) physiographic province. Box plot box is bounded by the 25th and 75th quartiles, and the horizontal line in the box is the median; box plot whiskers encompass all data between the 25th and 75th quartiles ±1.5× the interquartile range. Samples that fall outside the statistical range of the subsets are keyed to the dominant land use or by the physiographic province they are in. $^{10}Be_i$ erosion rate means are indistinguishable when grouped by land use (p values in panel A); when grouped by physiographic province, $^{10}Be_i$ erosion rate means are statistically indistinguishable, though right at the threshold of being different (p value in panel B), likely due to the lower

erosion rates in the Coastal Plain.

Figure 5. Log-log plot of $^{9}Be_{reac}$-normalized $^{10}Be_{m}$ concentrations shows no statistical inverse relationship to $^{10}Be_{i}$-derived sediment flux within the Potomac River basin as a whole, or by physiographic province.

Figure 6. Erosion indices (EIs) of sampled basins for which there are multiple decades of sediment yield data (Gellis et al., 2004) show more $^{10}Be_{m}$ export from headwater basins in the Appalachian Plateau (AP) and Valley and Ridge (V&R) and from the Piedmont (PIED), where agricultural land use is intensive. Individual panels (A–C) remove catchment overlap for visibility. EIs for each sampling site are valid for the entire upstream basin area. EI values are given in parentheses after each sample ID. Data from Brown et al. (1998) are indicated by U.S. Geological Survey (USGS) stream gauging station IDs. The Hybla Valley core site is indicated by the white star in panel A. The remainder of map symbology is the same as in Figure 1. BR—Blue Ridge, CP—Coastal Plain.

Figure 7. Mean ± 1σ standard deviations of $^{10}Be_{i}$-derived erosion rates for outcrops in the upper reaches of the Potomac River basin compared to basin-wide $^{10}Be_{i}$ erosion rates. Differences between erosion rates in the Appalachian Plateau provide evidence for relief growth over 10^4 yr timescales, but not in the Valley and Ridge or Blue Ridge Provinces, where outcrop and basin-averaged erosion rates overlap within 1σ uncertainties. Bedrock data for the Appalachian Plateau come from Hancock and Kirwan (2007), Portenga et al. (2013), and Reuter (2005); bedrock data for the Valley and Ridge come from Duxbury et al. (2015) and Portenga et al. (2013); bedrock data for the Blue Ridge come from Duxbury et al. (2015), Hancock et al. (2015), and Portenga et al. (2013). Basin-averaged data for the Appalachian Plateau come from this study; basin-averaged data for the Valley and Ridge and Blue Ridge come from this study and Duxbury et al. (2015).

Figure 8. $^{10}Be_{m}$ concentrations measured from samples taken from the Hybla Valley sediment core (circles) and from the modern-day Potomac River at POT01 (diamond), the furthest downstream, main river sample. Error bars on EIs are equal to the 1σ analytical uncertainty of the measured $^{10}Be_{m}$ concentrations, most of which are too small to be seen behind the data symbols. $^{10}Be_{m}$ measurements are connected by dashed black line for visibility only; the dashed black line does not indicate data continuity between samples. Results indicate that there is more erosion of topsoils, which are rich in $^{10}Be_{m}$, during colder climate periods and less erosion – lower $^{10}Be_{m}$ concentrations - during warmer climate periods. The age-depth relationship for the Hybla Valley core comes from Litwin et al. (2013). Solid gray line shows oak species abundance (*Quercus* spp.) and its changes through time, with decreases in abundance indicating colder climatic periods (Litwin et al., 2013).

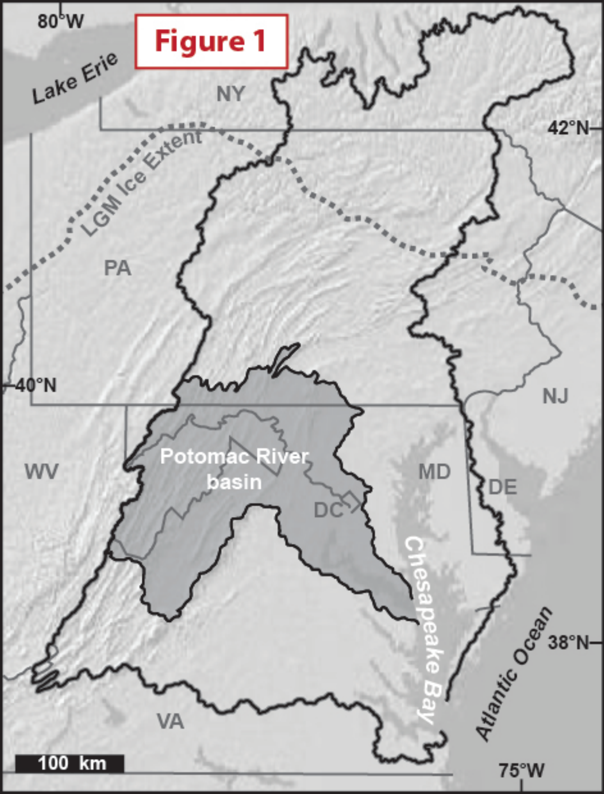

Figure 1
80°W
Lake Erie
NY
42°N
LGM Ice Extent
PA
40°N
NJ
Potomac River basin
WV
MD
DE
DC
Chesapeake Bay
Atlantic Ocean
38°N
VA
100 km
75°W

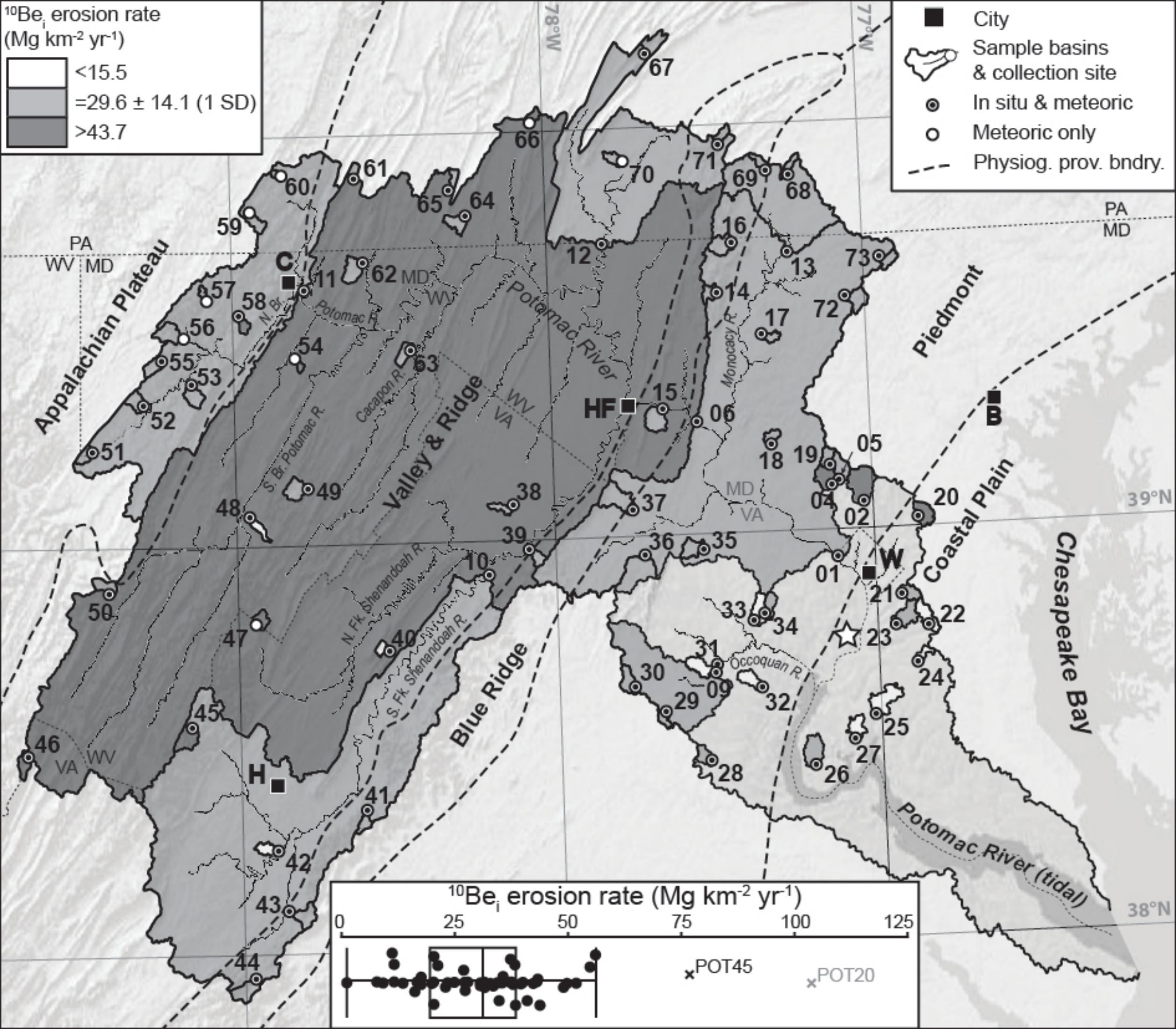

$^{10}Be_i$ erosion rate ($Mg\ km^{-2}\ yr^{-1}$)
<15.5
=29.6 ± 14.1 (1 SD)
>43.7
City
Sample basins & collection site
In situ & meteoric
Meteoric only
Physiog. prov. bndry.
78°W
77°W
39°N
38°N
PA
MD
WV
VA
Appalachian Plateau
Valley & Ridge
Blue Ridge
Piedmont
Coastal Plain
Chesapeake Bay
Potomac River
Potomac River (tidal)
N. Br. Potomac R.
S. Br. Potomac R.
Cacapon R.
N. Fk. Shenandoah R.
S. Fk. Shenandoah R.
Monocacy R.
Occoquan R.
C
HF
H
W
B
$^{10}Be_i$ erosion rate ($Mg\ km^{-2}\ yr^{-1}$)
0
25
50
75
100
125
POT45
POT20

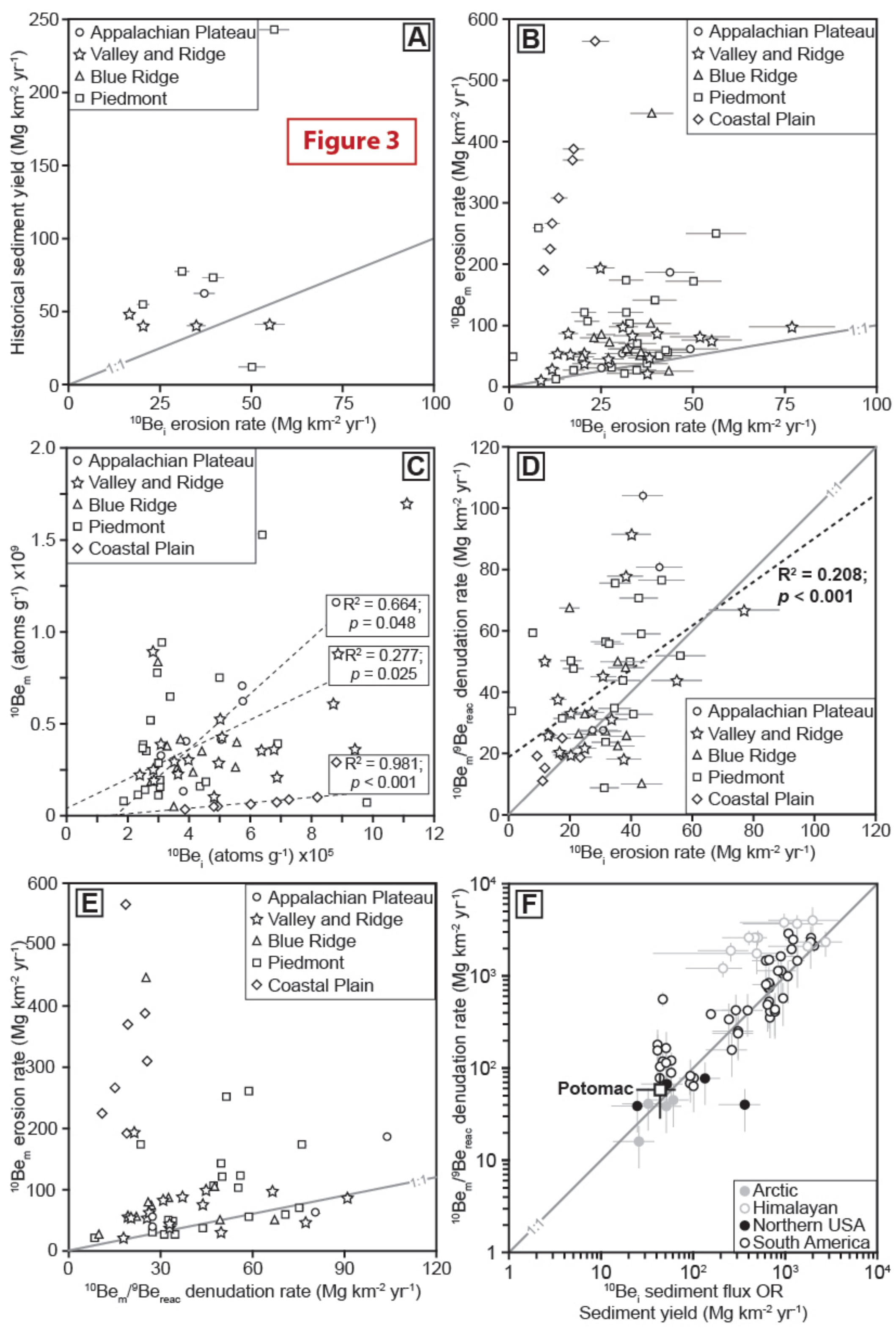
A
Appalachian Plateau
Valley and Ridge
Blue Ridge
Piedmont
Historical sediment yield (Mg km-2 yr-1)
10Be_i erosion rate (Mg km-2 yr-1)
1:1
B
Appalachian Plateau
Valley and Ridge
Blue Ridge
Piedmont
Coastal Plain
10Be_m erosion rate (Mg km-2 yr-1)
10Be_i erosion rate (Mg km-2 yr-1)
1:1
C
Appalachian Plateau
Valley and Ridge
Blue Ridge
Piedmont
Coastal Plain
10Be_m (atoms g-1) x10^9
10Be_i (atoms g-1) x10^5
R² = 0.664; p = 0.048
R² = 0.277; p = 0.025
R² = 0.981; p < 0.001
D
10Be_m/9Be_reac denudation rate (Mg km-2 yr-1)
10Be_i erosion rate (Mg km-2 yr-1)
R² = 0.208; p < 0.001
1:1
Appalachian Plateau
Valley and Ridge
Blue Ridge
Piedmont
Coastal Plain
E
Appalachian Plateau
Valley and Ridge
Blue Ridge
Piedmont
Coastal Plain
10Be_m erosion rate (Mg km-2 yr-1)
10Be_m/9Be_reac denudation rate (Mg km-2 yr-1)
1:1
F
10Be_m/9Be_reac denudation rate (Mg km-2 yr-1)
10Be_i sediment flux OR Sediment yield (Mg km-2 yr-1)
Potomac
1:1
Arctic
Himalayan
Northern USA
South America

Figure 3

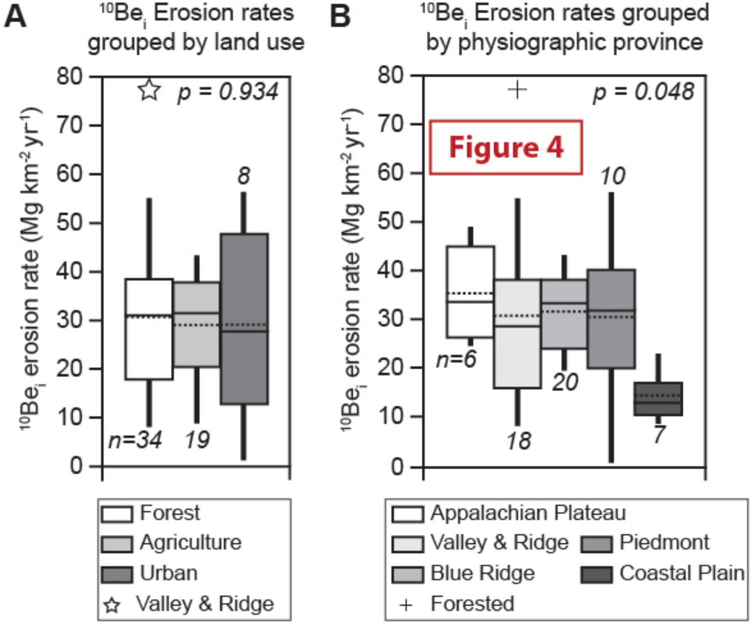

A
$^{10}Be_i$ Erosion rates grouped by land use
p = 0.934
$^{10}Be_i$ erosion rate ($Mg\ km^{-2}\ yr^{-1}$)
80
70
60
50
40
30
20
10
0
n=34
19
8
Forest
Agriculture
Urban
Valley & Ridge
B
$^{10}Be_i$ Erosion rates grouped by physiographic province
p = 0.048
Figure 4
n=6
18
20
10
7
Appalachian Plateau
Valley & Ridge
Piedmont
Blue Ridge
Coastal Plain
Forested

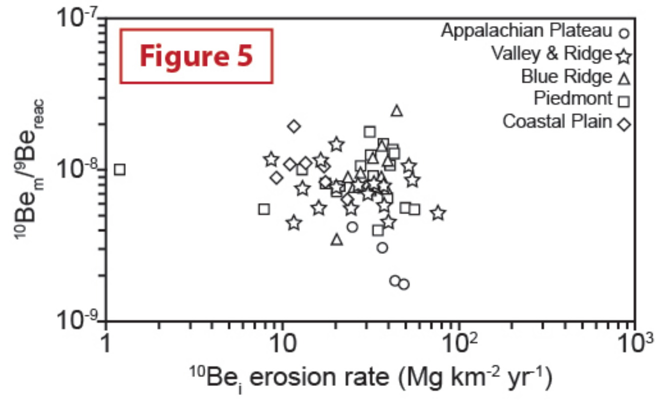

Figure 5
Appalachian Plateau
Valley & Ridge
Blue Ridge
Piedmont
Coastal Plain
$^{10}Be_m/^9Be_{reac}$
10^{-7}
10^{-8}
10^{-9}
1
10
10^2
10^3
$^{10}Be_i$ erosion rate (Mg km^{-2} yr^{-1})

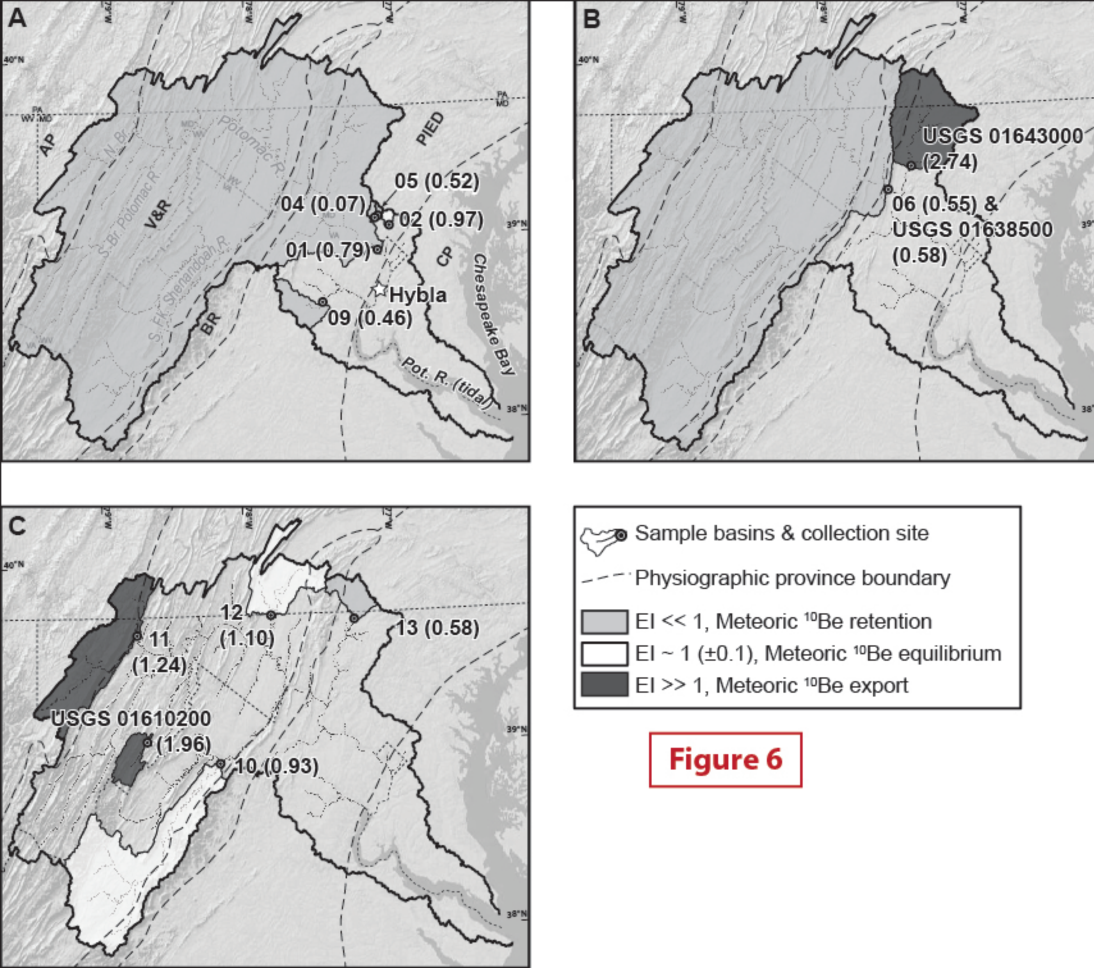
A
B
C
AP
PIED
V&R
BR
CP
N. Br.
Potomac R.
S. Br. Potomac R.
S. Fk. Shenandoah R.
Pot. R. (tidal)
Chesapeake Bay
Hybla
04 (0.07)
05 (0.52)
02 (0.97)
01 (0.79)
09 (0.46)
USGS 01643000 (2.74)
06 (0.55) &
USGS 01638500 (0.58)
11 (1.24)
12 (1.10)
13 (0.58)
USGS 01610200 (1.96)
10 (0.93)
Sample basins & collection site
Physiographic province boundary
EI << 1, Meteoric 10Be retention
EI ~ 1 (±0.1), Meteoric 10Be equilibrium
EI >> 1, Meteoric 10Be export

Figure 6

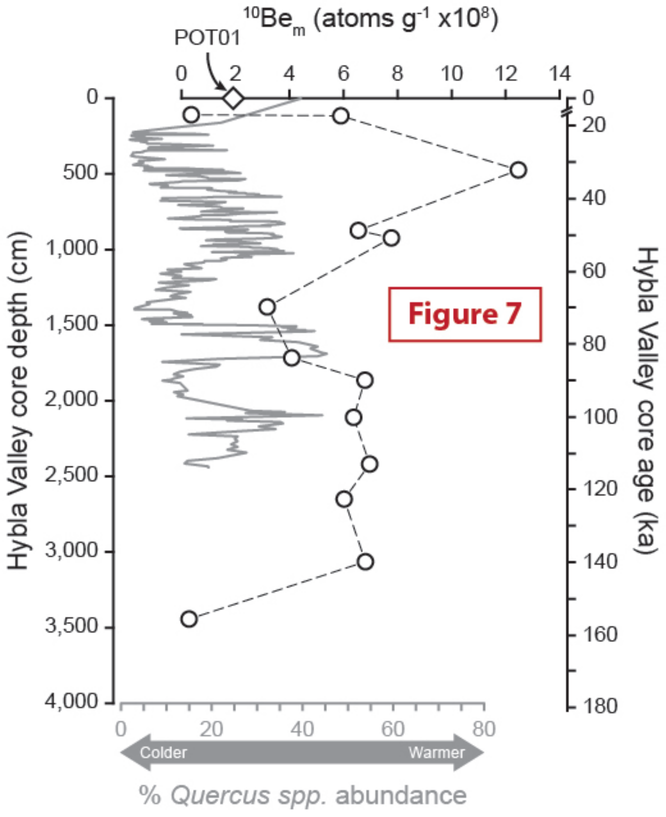

$^{10}Be_m$ (atoms g^{-1} x10^8)
POT01
0
2
4
6
8
10
12
14
0
500
1,000
1,500
2,000
2,500
3,000
3,500
4,000
Hybla Valley core depth (cm)
0
20
40
60
80
100
120
140
160
180
Hybla Valley core age (ka)
Figure 7
0
20
40
60
80
Colder
Warmer
% *Quercus spp.* abundance

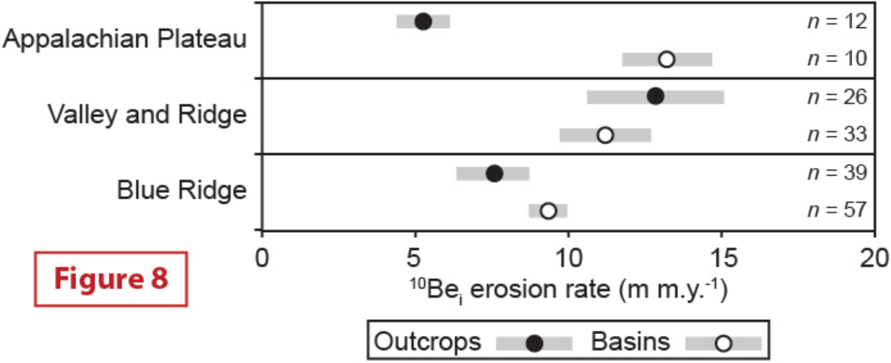
Appalachian Plateau
Valley and Ridge
Blue Ridge
n = 12
n = 10
n = 26
n = 33
n = 39
n = 57
0
5
10
15
20
$^{10}Be_i$ erosion rate (m m.y.$^{-1}$)
Outcrops
Basins

Figure 8